

LEVEL

12
B.S.

AD

AD A095110

**SPRAY MODELLING FOR MULTIFUEL
ENGINES**

First Annual Technical Report

by

ELKOTB, M.M.

Professor of Combustion

Cairo University

July 1980

SDTIC
ELECTE
FEB 17 1981
D
C

EUROPEAN RESEARCH OFFICE

United States Army

London

England

GRANT NUMBER DA - ERO - 79 - C - 0017

CAIRO CENTER FOR COMBUSTION (EGYPT)

Approved for Public Release - Distribution Unlimited

BBC FILE COPY

81 2 17 037

AD

(16)

SPRAY MODELLING FOR MULTIFUEL ENGINES.

12) 72

9) First Annual Technical Report, No. 1, Mar 79-Apr 80

by **ELKOTB, M.M.**

Professor of Combustion
Cairo University

11) July 1980



(16) 1T161203.BH37

(17) 06

12) 4. 4. / ELKOTB

EUROPEAN RESEARCH OFFICE

United States Army

London

England

(15)

GRANT NUMBER DA - ERO - 79 - G - 0017

CAIRO CENTER FOR COMBUSTION

Approved for Public Release : Distribution Unlimited

39475

CONTENTS

	Page
- Acknowledgments	2
- Summary	3
- List of Figures	4
- CHAPTER 1 Introduction	6
- CHAPTER 2 Influence of various physical properties of fuel on mixing and combustion processes.	9
- CHAPTER 3 Object of the present work	24
- CHAPTER 4 Spatial variation of Heat Transfer in Swirl Combustion Chambers	28
- CHAPTER 5 Prediction and measurement of Flow in Motored Diesel Engines swirl chambers	55
- Conclusions.	74

Accession For	
NTIS GRA&I	<input checked="" type="checkbox"/>
DTIC TAB	<input type="checkbox"/>
Unannounced	<input type="checkbox"/>
Justification	
By _____	
Distribution/ _____	
Availability Codes	
Dist	Avail and/or Special
A	

ACKNOWLEDGEMENT

The authors are appreciative of the financial support for this work which was provided by THE EUROPEAN RESEARCH OFFICE through Grant Number DA-ERO-79-G-0017.

Thanks also are due to Dr. ALY, S.L. for his valuable suggestions during the preparation of this report.

S U M M A R Y

The present project deals with the fuel spray modelling in multifuel engines using the droplet behaviour approach. The multifuel engine is able to burn different types of fuel having various physical and chemical properties, either clear or mixture with arbitrary mixing ratio. Analysis of the physical and chemical properties affecting mixture creation and combustion have been carried out to define the parameters affecting the accuracy of spray modelling. It is found that the spray is affected by air flow field, heat transfer, fuel atomization, droplet behaviour, fuel evaporation and chemical kinetics. Solution of the flow field and experimental results of heat transfer have been obtained.

Experiments were performed in a set up that allowed variation of the swirl chamber geometry and operating conditions to evaluate the instantaneous surface heat transfer under firing conditions. The instantaneous heat flux was determined taking into consideration the instantaneous composition of products and variation of specific heats. A generalized expression has been established for the calculation of heat transfer to the chamber wall under variable design and operating conditions.

Prediction of the air flow field is based on the solution of the finite difference analogue of the governing differential equations for the transport of mass, momentum and energy. The $k-\epsilon$ model of turbulence has been used. A special technique has been established to satisfy compressibility, local continuity and reduce the mass source at each grid node to zero. Measurements of air flow field are carried using a hot wire anemometer. Agreement between predictions and measurements is fairly good, which confirms the accuracy of the prediction procedure.

LIST OF FIGURES

		Page
Fig.1	Behaviour of diesel engine with diesel fuel and gasolene	14
Fig.2	Comparison between diesel engine and multifuel engine working with diesel fuel and gasolene	16
Fig.3	Precombustion chamber (MWM) for multifuel engine	18
Fig.4	Swirl combustion chamber for multifuel engine (engine Hispano Swiss production)	19
Fig.5	Spherical combustion chamber in piston for multifuel engine (M.A.N.)	20
Fig.6	Speed characteristic of diesel engine Nasr working with diesel fuel, Gasolene 70 ON and mixture of gasolene and diesel fuel 50/50%	22
Fig.7	Speed characteristic of diesel engine Nasr working with kerosene and Jet kerosene	23
Fig.8	Scheme of experimental set up for heat transfer study	32
Fig.9	Schematic drawing of the swirl chamber for heat transfer study	33
Fig.10	The courses of swirl chamber gas pressure, fuel pressure, needle lift and the location of TDC in relation with time	35
Fig.11	Relation between mean wall temperature and engine speed for different swirl chamber volume ratios at full load	41
Fig.12	Relation between mean wall temperature and engine speed for different throat diameter of the tangential channel at full load	42
Fig.13	Relation between mean wall temperature and engine speed for different inclination angles of the tangential channel at full load	43
Fig.14	Relation between mean wall temperature and engine speed for different opening pressures of the injector at full load	44
Fig.15	Effect of varying swirl chamber volume on rate of heat release	45
Fig.16	Effect of varying swirl chamber volume on heat transfer coefficient and surface heat flux	47
Fig.17	Effect of varying throat diameter of the tangential channel on heat transfer coefficient and surface heat flux	48

	Page
Fig.18 Effect of varying inclination angle of tangential channel on heat transfer coefficient and surface heat flux	49
Fig.19 Effect of varying pressure on heat transfer coefficient and heat flux	50
Fig.20 Relation between Nusselt Number and $\left \text{Re}^{0.5} (d_s/d_t)^{1.2} \right / \left P_r^4 E_u^{1.5} \right $	51
Fig.21 Comparison between experimental work and empirical correlation	52
Fig.22 Scheme of experimental set up for Air flow measurements	59
Fig.23 Scheme of the test combustion chamber for air flow measurements	60
Fig.24 Computational grid	64
Fig.25 Velocity vector plot during compression stroke	64
Fig.26 Velocity vector plot during expansion stroke	68
Fig.27 Turbulence intensity contours during compression stroke	68
Fig.28 Photography of the flow field at T.D.C.	68
Fig.29 Predicted and measured tangential velocity in plane 2 at various radii at 20° BTDC	70
Fig.30 Predicted and measured tangential velocity during compression in plane 2 at 10 mm from inside surface	70
Fig.31 Radial turbulence intensity distribution in plane 2 at 20° BTDC	71
Fig.32 Turbulence intensity during compression at 10 mm from inside surface.	71

CHAPTER I

INTRODUCTION

The multifuel engine, which is able to burn different types of fuel either clear or mixtures with arbitrary mixing ratio, is required to ease the problem of disproportion between consumption and production of diesel fuel. It must be able to satisfy burning of liquid fuels of wide distillation range, and preserve the same power output and specific fuel consumption at various speeds and loads. Therefore, the fuel system must secure reliable delivery of fuel into engine, good mixture creation, good ignition, smooth burning with minimum emissions and minimum corrosion of engine elements. In addition easy starting of engine must be secured.

The multifuel engine has been known at the beginning of the development of combustion and represented by the engine IANZ-BULDOG having a hot bulb. However, some design difficulties at that time have stopped their development for many years. A lack of some kinds of fuel for combustion during World War II and the increase of diesel fuel consumption due to its use in various fields have urged the resumption of the development of multifuel engine. A multifuel piston combustion may be designed on the basis of either a gasoline engine or diesel engine. However, one has to say that the diesel engine suits more the multifuel operation since it works with higher compression ratio as well as with fuel injection in the cylinder which appears to be necessary conditions for combustion of heavier kinds of fuel. Moreover, the reliability and economy of diesel engines have been acknowledged.

In the early stages of the development of modern high speed diesel engines the varieties of combustion chamber layouts were numerous. There is no doubt that this early intensive work resulted in better stabilization of combustion using two types of combustion chambers, namely the open chambers and the divided ones with their basic three categories; the prechambers, the air cells and the swirl combustion chambers. The multifuel engine must be prepared with a combustion chamber controlling combustion of fuel during the period of rapid pressure rise to obtain better burning characteristics. That is why most of designers used either precombustion chamber or swirl one with high temperature steel inserts to preserve the chamber temperature and consequently shorten the ignition delay. Actually swirl chambers with high temperature steel inserts are suitable for burning multifuel.

This shows why the air-fuel mixing process prior to autoignition is important in multifuel engines in general and in swirl chamber multifuel engines in particular. The principle

of burning in swirl chamber being injection of fuel across a rapidly rotating mass of air in the combustion chamber in such a manner that the air has to find the fuel. In this case the mixing process includes transport of fuel from the spray by the swirling air flow, deflection of the fuel spray, impingement of the spray on the combustion chamber wall and the formation of turbulence at the separation boundaries of the air Jet in the swirl chamber. Besides, the impinged Jet spread on the combustion chamber wall forming a fuel film of very small thickness. This film takes its required heat of evaporation from the wall and surroundings by convection.

The analytical solution of the mixing process resulting from the space and film mixture creation inside swirl combustion chambers is complex. Many investigators have studied the problem of mixture formation and combustion in diesel engines, but most of them treated the problem either in general or by formulating some empirical relations to represent the individual processes. Only few investigators have tried to formulate the mixture formation process and combustion in the swirl chamber on the basis of some known physical laws.

Along this line the present project is conducted to deal with a theoretical model and experimental verification of the fuel spray trajectory in multifuel engines using swirl combustion chambers. This spray modelling is required to investigate speedily and with reasonable details and accuracy the combustion of fuel having various physical and chemical properties and to study the development of multifuel engines. The fuel mixture creation and combustion are generally affected by the air flow field, heat transfer, fuel atomization, droplet behaviour, fuel evaporation, chemical kinetics, delay period and combustion chamber shape. The mathematical model, which includes all these factors, can give quite sufficient accurate results. These factors have been solved in successive stages.

In this first Annual Technical report, analysis of the physical properties affecting mixture creation and combustion in multifuel engines, solution of the air flow field and heat transfer in swirl chambers have been dealt with. The governing conservation equations of the dimensional flow field in the swirl chamber have been formulated. The $k-\epsilon$ model of turbulence has been used to define the turbulent viscosity and the turbulent exchange coefficient. The equations are solved using the finite difference technique in which the compressibility and local continuity were satisfied. A special technique has been established to reduce the mass source at each grid node to zero. An experimental plant has been built to measure the flow field in an actual swirl chamber using the hot wire anemometer. A comparison over a wide range of data is required to validate the mathematical model. The solution

of the flow field has been conducted by Prof. ELKOTB, M.M. , Dr. ABOU-ALLEIL, M.M. and Eng. SALEM, S.

The instantaneous surface heat transfer in swirl combustion chamber of various geometry has been determined experimentally under firing conditions. Generalized expressions have been established for the calculation of heat transfer to the chamber wall under variable design and operating conditions. Prof. ELKOTB, M.M., Dr. AWAD, M.M. and Eng. ESMAIL are responsible for this part of the report.

The analysis of the influence of fuel properties on mixture creation and consequently the engine performance together with the preliminary measurement of engine performance when burning multifuel have been conducted by Prof. ELKOTB, M.M. and Dr. ELGOHEIMY, M.N.

Experimental set ups for the investigation of other mentioned important parameters have been built up. Their details together with the results will be discussed in other Technical Reports.

CHAPTER 2

INFLUENCE OF PHYSICAL PROPERTIES OF FUEL ON MIXING AND COMBUSTION PROCESSES

2-1 INTRODUCTION

The multifuel engine must satisfy the common demands of all engines such as high specific power output, high economy, minimum size and weight, high reliability and easy maintenance. Moreover, it must be able to meet further important demands as follows :

a- to enable combustion of liquid fuel of both natural and synthetic origin of wide distillation range, + 30°C to 450°C. i.e gasoline, Kerosene, aviation fuel, Diesel fuel and even all kinds of lubricating oils.

b- to preserve approximately the same power output and operating characteristics for all fuels.

At the same time the multifuel engine must operate in the same way when using either clear fuels or mixtures with any arbitrary ratio. Table 2.1 shows the physical and chemical properties of main Fuels produced in Egypt. It is evident from this table that the fuels to be used in multifuel engines possess various physical properties which affect the mixing and combustion processes differently. Therefore, the fuel system must secure reliable delivery of fuel into engine, good mixture creation, good ignition, smooth burning with minimum emission and minimum corrosion of engine elements. In addition easy starting of engine must be secured. These demands being laid upon multifuel are not small and their successful fulfilment strikes at present with several difficulties. A brief analysis of various physical properties of the mentioned fuel will be carried out to explore their effects on the engine performance.

2-2 ANALYSIS OF VARIOUS PHYSICAL PROPERTIES

a- Low distillation temperature of light fuels: light fuel such as gasoline and aviation fuel will cause vapour lock due to evaporation of light fractions. This may happen in the low pressure branch of the fuel system when exposed to high temperatures from the engine and causes an irregular, interrupted and incorrect metering of fuel. Restarting of warm engine will be interrupted when using light fuels as the fuel will evaporate as a result of the high temperatures achieved. The temperatures of the fuel system may reach a value of about 50°C or more (up to 60°C) exceeding the initial distillation

TABLE 2.2
Basic Physical-Chemical Properties of Fuels of Egyptian Production

Fuel Ch _{cs}	Engine Fuel	Misir Gas Oil	Misir Motor Gasoline 70 Octane	Misir Motor Gasoline 85 Octane	Misir Excellent Kerosene	Misir Kerosene
Net calorific value (Kcal/kg).	10550	10400	10400	10400	10250	10250
Specific gravity at 15/4°C	0.82+0.87 min.	0.76 max.	0.76 max.	0.76 max.	0.778 max.	0.82 max.
Kinematic viscosity at 20°C (cotl).	4 + 6	0.65 + 0.8	0.65 + 0.8	0.65 + 0.8	2.5 + 3.5	2.5 + 3.5
Cetane No.	45	25	19	37		38
Fract- ional	10	12.6	13.2	20		22
Composi- tion	3	13.8	13.5	73.3		
Final boiling point (°C)	87	74.6	205	205	290 + 300	290 + 300
Reid vapour pressure torr (kp/cm ²)	0.17	0.63 + 0.77	0.63 + 0.77	0.63 + 0.77	0.25 + 0.30	0.25 + 0.30
Diesel index (D.I).	min. 48	15	6	29	70	30
Temperature of initial distilla- tion (°C).	90	30	30	70		70
Temperature of spontaneous igni- tion (°C).	--	--	--	--	--	--
T.E.L. Contents, (me/IG).	ml	1.5	3.8	ml	ml	ml

temperature. This difficulty of operation increases with the increase of the atmospheric temperature, the condition of operation most prevailing in Egypt.

The temperature of the fuel delivery parts must not exceed 40°C if vapour lock is to be prevented. More effective fuel delivery pump which delivers greater quantity of fuel, is required in multifuel engines as the flow of fuel cools the fuel pump intensively. Thus, to secure the good ability of restarting of warm engine it would be beneficial to equip the fuel system with an electric delivery pump, which is independent on the drive from the engine. The increase of the delivery pressure of fuel to 1.5 up to 3 bar will also limit the tendency to create vapour lock.

b- Low viscosity of lighter fuels.

Low viscosity of fuel is obtained when using light fuels. This causes leakage of fuel through clearances in injection units resulting in incorrect metering of fuel. In addition excessive atomization of fuel is obtained causing small fuel penetration, lack of homogeneity and burning in the vicinity of the injector. This may cause overheating, carbonization and deformation of some parts. Moreover, the lubrication of the moving elements of the pump decreases causing excessive wear.

Leakage of light fuels can be prevented either by oil sealing rings or by manufacturing special grooves on plunger in which the fuel may sedimentate and then gets drained into the suction part of the pump. The injection pump must also be supplied with lubricating oil from the engine to decrease the wear of its moving parts.

c- Low value of cetane number.

Light fuels have low values of cetane number in comparison with diesel fuel, creating the following difficulties :

- i, high self ignition of fuel as well as high delay period.
- ii, hard running and difficult starting of the engine due to small compression temperature.

The cetane number of the fuel depends on both the chemical and fractional composition of fuel. The alkaline hydrocarbons have the highest cetane number while the aromatic hydrocarbons have the lowest cetane number. Cyclones have middle values between alkalines and aromatics. Lighter fuels have small cetane number resulting in difficult ignition of fuel when used in diesel engines. However, high cetane fuels possess low ignition delay and burn in the vicinity of the injector. That is why the air present far away from the injector does not take part in the burning process and consequently incomplete burning of fuels may occur.

This causes smoky combustion and drop of engine economy.

The problems of hard running and long delay period are one of the main difficulties of multifuel engines working with various liquid fuels. The analysis of these problems and the possibility of their solution will be dealt with later on.

c- Saturation fuel pressure.

It is known that the saturation pressure of the fuel characterizes the evaporation of fuel. The REID pressure of the diesel fuel is zero while it may achieve a value of 100 torrs for petrol fuel. Thus the saturation pressure increases with the increase of light fractions. The increase of saturation pressure causes an excessive creation of vapour lock. Moreover, small amount of heat is required to evaporate the same quantity of fuel, it is required to use fuels of REID pressure not exceeding 450 torr.

d- fractional composition of fuels.

The fractional composition of fuels affects directly the ability of fuel to evaporate, atomize and disperse. The time of evaporation in high speed diesel engines is very short. It is, therefore, necessary for both light and heavy fractions contained in diesel engine fuels to be in a suitable ratio. Heavy components of fuel evaporate slowly and imperfect combustion is obtained leading to smoke and soot concentration in the exhaust gases. Consequently, the engine efficiency decreases.

While evaporation of light components is quicker, their point of inflammation is higher than that of heavier components. A greater quantity of light components in fuels may cause high fuel concentration in the zones behind the injector. This may cause high increase of pressure rate and overheating, resulting in hard running of engine.

e- change of calorific value and specific weight of various fuels.

The change of calorific value is not substantial as it does not exceed 3%. However, the specific weight varies by 10 up to 15%. The decrease of the specific weight causes a decrease of the quantity of fuel injected and consequently a decrease of the output power from the engine and engine economy.

Therefore, the injection pump of multifuel engine must be equipped with an arrangement for changing the injected quantity independence of the fuel specific weight.

The effect of fuel density change is considerably lower than that of viscosity. However, they must be considered together with their change in the operating temperature when

selecting the holes of the injectors.

2-3 MULTIFUEL COMBUSTION IN DIESEL ENGINES

Combustion of fuels in diesel engines is a very complicated problem. Fuel inflammation occurs from the heated up air in the combustion chamber. For that reason compression ratio of more than 13 is necessary to create convenient conditions for burning before TDC. The fuel is injected in the combustion chamber with an injection advance ranging between 20 to 40 degrees before TDC according to the engine speed. Thereafter the ignition takes place after a period of time equivalent to 10-20 degrees of the crankshaft. The variation of gas pressure inside the cylinder with crankangle for gasoline and diesel fuel is shown in Fig.(1). The preparation of fuel for combustion is responsible for the ignition delay period. The whole process of burning as well as the performance of the engine depends on the ignition delay period. The quantity of fuel delivered during the delay period will start to burn directly after creation of active centres. It follows that the longer the delay period is the more quantity of fuel is accumulated in the combustion space and then rapid increase of pressure is obtained. Hard operation of the engine is obtained when the rate of pressure rise (roughness of combustion) exceeds 6 bar/degree crank. This increase of pressure rise rate is accompanied by excessive wear of bearing, crankshaft and rumbling sound. High hard operation of the engine is also accompanied by smoke outlet, and high specific fuel consumption.

From the above can be seen that increasing the delay period increases the hardness of diesel engine work while decreasing it makes the engine operation softer. However, having too small, a delay period and at the same time long fuel delivery period, lead to imperfect combustion, and soot is obtained in the exhaust. The ignition delay period is divided into physical and chemical delay periods which overlap each other.

The fuel atomization, partial evaporation and heating up of vapours to the inflammation temperature occur during the physical delay period. The formation of active centres and oxidation occur during the chemical delay period. The physical ignition lag has a considerable value when using heavy fuels. It is evident from Fig.1 that the ignition delay of gasoline burnt in diesel engine is considerably higher than that of diesel fuel and consequently hard operation is obtained. Therefore, a normal diesel engine is not suitable to work with gasoline. The multifuel engine must satisfy the

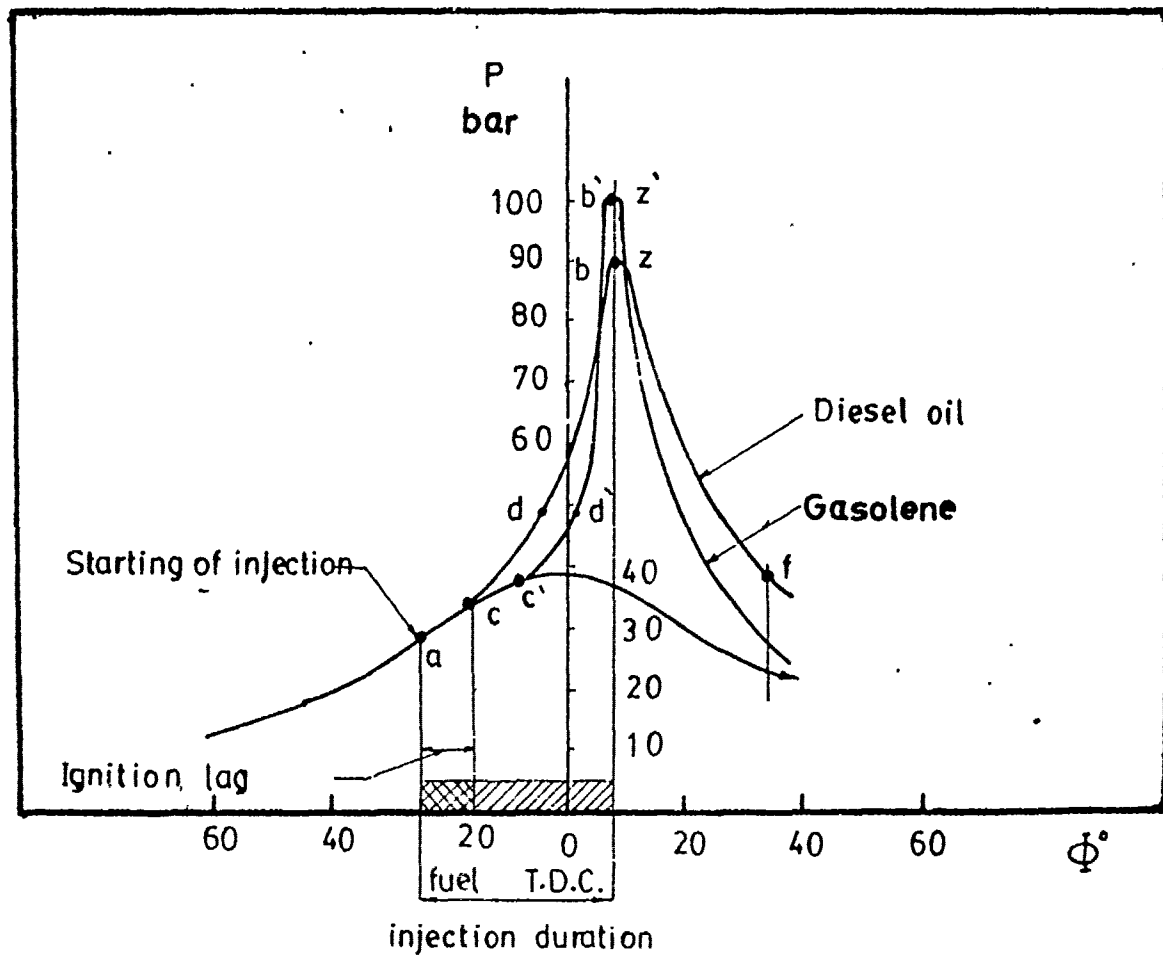


FIG.1 BEHAVIOUR OF DIESEL ENGINE WITH DIESEL FUEL AND GASOLENE.

same pressure variation as shown in Fig.2. A method must be found to remove the quick increase of pressure of the uncontrolled part (c'd') on the diagram. Therefore, it is required to control the ignition delay period. To try to solve this problem it is required to define accurately the influence of various factors on the delay period.

The delay period is influenced by the kind of fuel, oxygen concentration, concentration of residual gases and presence of catalyzers and admixtures.

The parafinic hydrocarbons have the shortest ignition delay due to the long chain structure while aromatics have the longest ignition delay due to their ring structure. Therefore, in comparison with the standard diesel fuel the ignition of Kerosene is somewhat greater, its increase of pressure smoother and maximum pressure smaller. On the contrary, gasolene (aromatic) has a long delay period thus increase of medium pressure is sharp and the maximum pressure is high. The self-ignition temperature of various kinds of fuel were found to be

gasolene	470°	-	530 °C
Jet fuel (aviation kerosene)	240°	-	380 °C
diesel fuel	250	-	270 °C

Fuels with low self ignition temperatures such as kerosene and diesel fuel are suitable for burning in diesel engines.

The increase of oxygen concentration in mixture from 20% to 33% decreases the ignition delay from 80×10^{-4} sec to 55×10^{-4} sec. The change of ignition delay with oxygen concentration is approximately linear. Therefore the use of oxygen improves the engine starting as well as combustion.

It is also known that a great number of physical factors are affecting the delay period such as evaporation characteristics of fuel, its viscosity, air temperature at the end of compression, fresh charge temperature and density, air swirl and heat transfer in combustion chamber. For high speed engines heavy fuel has no time to evaporate.

The increase of turbulence intensity increases the quantity of heat transferred to the cylinder wall, resulting in a decrease of pressure and temperature of gases at the end of compression stroke. This decrease of temperature increases the delay period. At the same time the increase of turbulence intensity improves the fuel atomization, heat transfer to fuel droplets and evaporation, resulting in a decrease of the delay period. Therefore, it is possible to say that the ignition delay is shortened with the increase of the turbulence intensity.

P bar

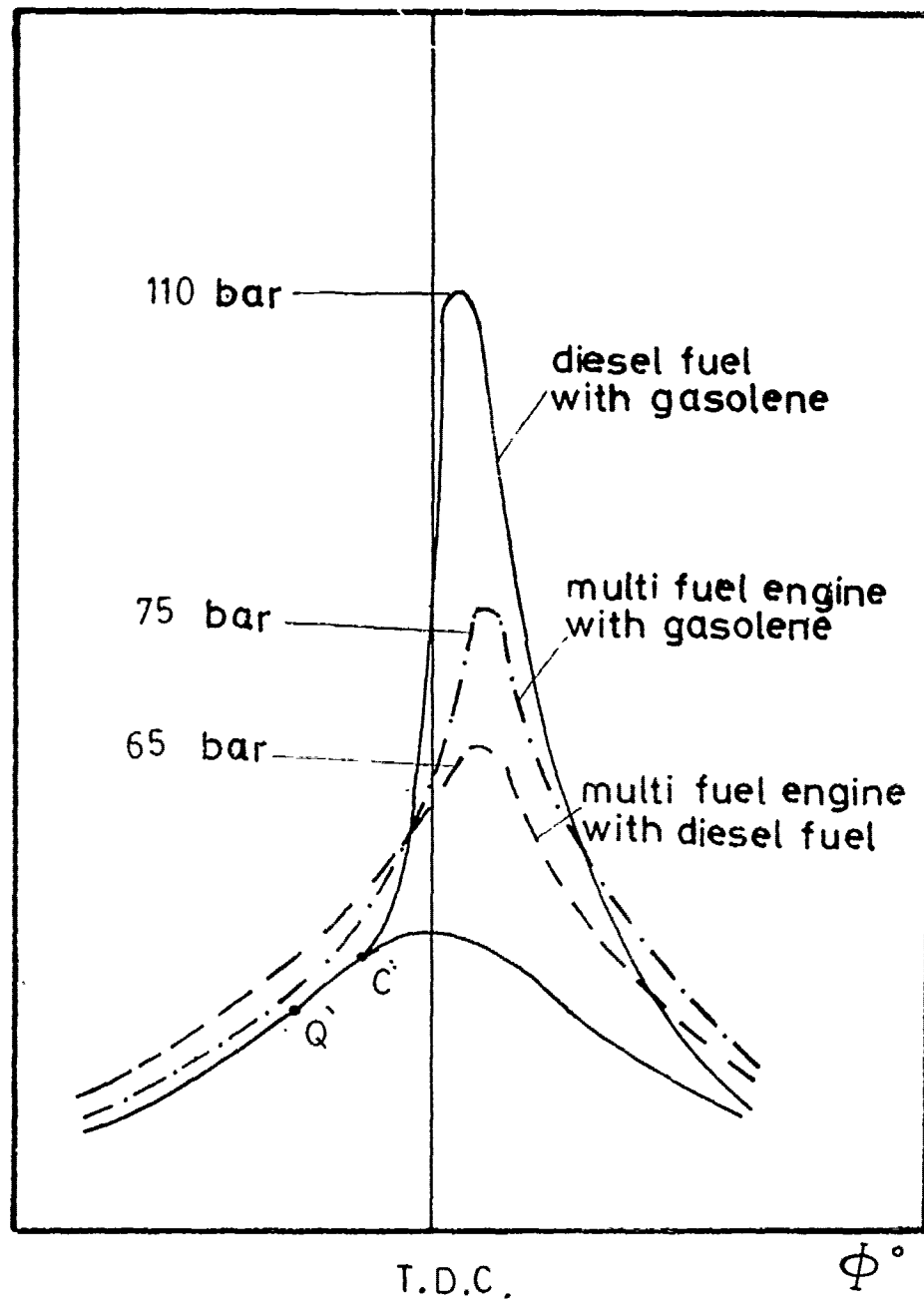


FIG.2

COMPARISON BETWEEN DIESEL ENGINE AND MULTIFUEL ENGINE WORKING WITH DIESEL FUEL AND GASOLENE.

The injection pressure is one of the factors that determines the quality of fuel atomization. The increase of fuel pressure decreases the fuel droplets diameter and consequently the total surface of fuel drops increases. This increases the heat exchange to fuel and relative oxygen concentration on the surface of fuel droplets, thus accelerating the physical-chemical preparation of fuel for ignition. The law of fuel delivery has no effect on the ignition delay. The change of fuel delivery causes a change of the fuel delivered per crank angle and leads to the change of heat release rate and, consequently, the pressure-time diagram. The number and size of injecting nozzle as well as the location of the injector have a substantial effect on the fineness and uniformity of atomization. However, there will be a substantial effect on the spray length inside the combustion space.

Finally it is evident that gasoline burning in diesel engines requires an increase of compression ratio, higher operating temperatures, avoidance of creation of vapour lock and regulation of fuel quantity.

2-4 CONTROLLING COMBUSTION OF MULTIFUEL

From the analysis of the factors affecting the delay period it is evident that the compression ratio, combustion chamber shape and design, method of mixture creation and initial conditions to engine have valuable importance when designing the multifuel engine. Moreover, the control of the course of burning has a direct effect on the performance of multifuel engine. Controlling the course of burning to secure multifuel combustion has been satisfied by shortening the delay period, regulating the combustion of fuel during the rapid pressure rise period and mixture creation in the combustion chamber space. That is why most of the designers used either precombustion chambers as shown in Fig.3 or swirl chambers as shown in Fig.4. These chambers are equipped with hot surfaces and thermal insulations to preserve the chamber temperature at high values sufficient to shorten ignition delay of aromatic fuels. Precombustion chambers are used by Daimler-Benz and M.A.N factories. Swirl combustion chambers are used by Deutz in their multifuel engines. The English multifuel engines are in most cases two stroke engines with opposite pistons (Leyland, Rolls-Royce, Commer and Country Climax).

Air cell with two holes injector can also be used. Part of the fuel is directed tangentially on the wall while the other part is directed towards the centre. Such combustion chamber is used by MAN Factory, Fig.5. Five percent of the injected fuel is directed tangentially on the wall of the spherical combustion chamber located in the piston.

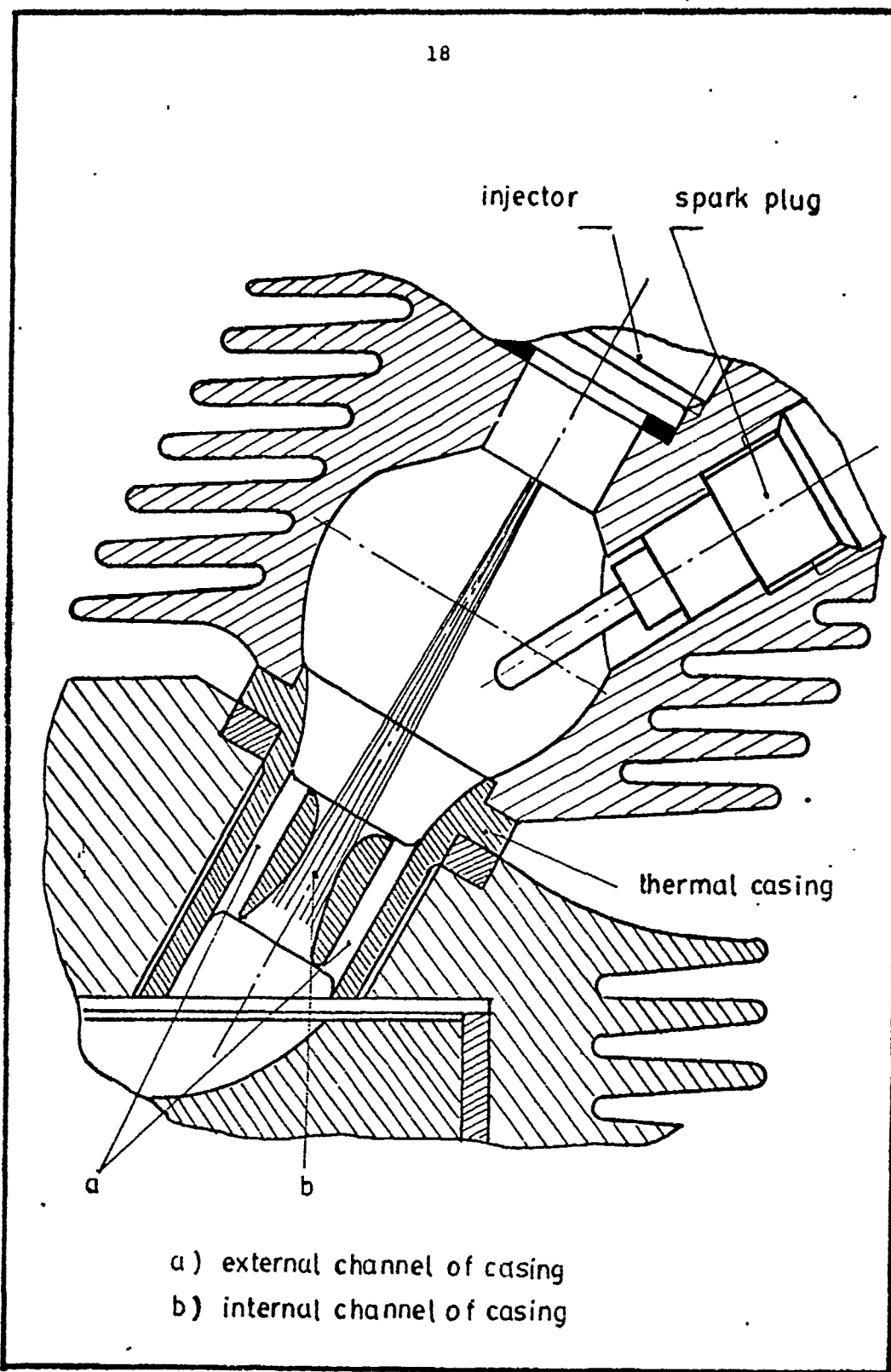


FIG.3 PRECOMBUSTION CHAMBER (MWM) FOR MULTIFUEL ENGINE

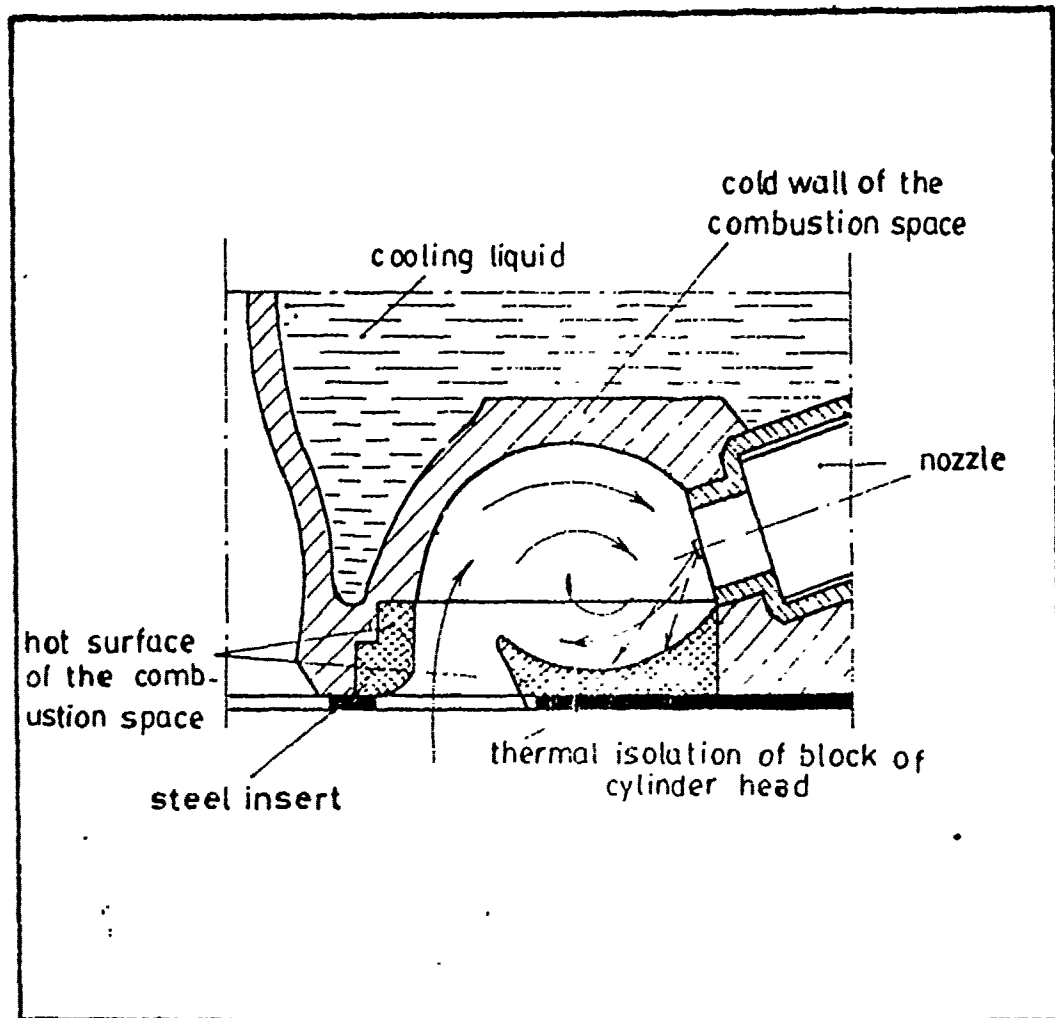


FIG.4 SWIRL COMBUSTION CHAMBER FOR MULTIFUEL ENGINE (ENGINE H.SPANO SWISS PRODUCTION)

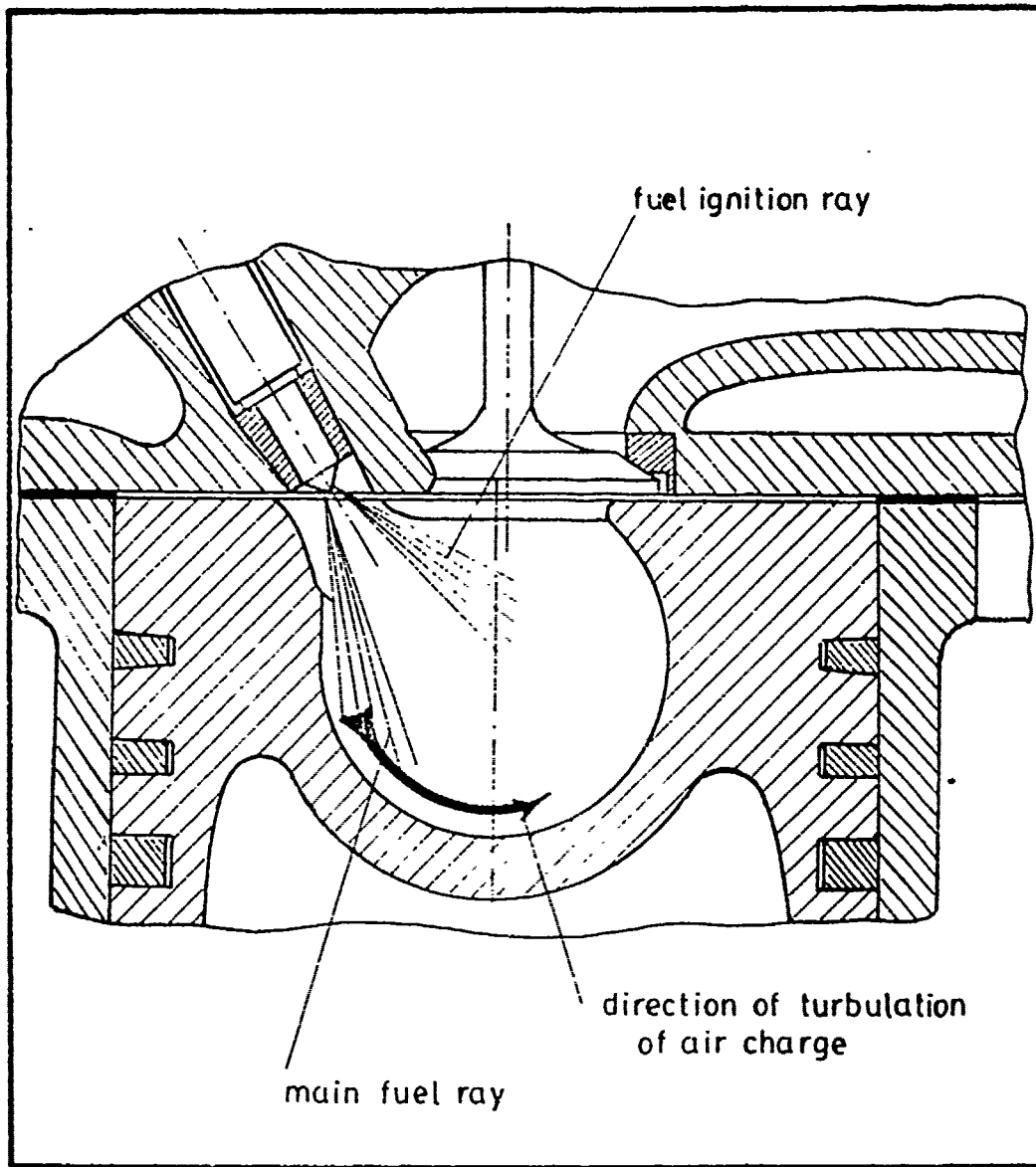


FIG.5 SPHERICAL COMBUSTION CHAMBER IN PISTON FOR MULTI FUEL ENGINE (M.A.N.)

2-5 PRELIMINARY RESULTS OF BURNING VARIOUS FUELS IN A DIESEL ENGINE

It was clear from the previous analysis that the engine performance was influenced by various factors affecting the mixture creation during the delay period. It is therefore required to measure the engine performance when burning either clear fuel or mixtures of arbitrary ratio. This is required to define the object of this work.

An Egyptian made diesel engine, Nasr 92-0501, was used for this purpose. It is a stationary, water cooled, four stroke, 2-cylinder engine. The main data of this engine are given in Table 2. The cylinder head is provided with a precombustion chamber. Pintle type injector with opening pressure of 130 bar was used to inject the fuel at an injection advance angle of 18 degrees before TDC. The engine was equipped with the required instrument for measuring the operational condition and the engine performance. A hydraulic dynamometer was used to measure the brake power. The exhaust gas temperature was measured by a Fe-constantan thermocouple. The measurement of smoke of exhaust gases was carried out by the through-flow gas analyser type Hartrige.

The tests have been carried out with the following fuels; diesel fuel $\rho = 0.842 \text{ gm/cm}^3$, gasolene 70 O.N $\rho = 0.732 \text{ gm/cm}^3$, Kerosene $\rho = 0.8115 \text{ gm/cm}^3$, jet Kerosene $\rho = 0.811 \text{ gm/cm}^3$ and mixture of diesel oil and gasolene $\rho = 0.789 \text{ gm/cm}^3$. The injection pump was adjusted according to the producer recommendation to give 8.5 cm^3 for 100 strokes at a speed of 500 RPM. Some of the results obtained for the performance of the engine when burning the mentioned fuels are illustrated in Fig.6. It was found that the power decreased, the specific fuel consumption increased and the smoke decreased with the increase of the gasolene ratio in the diesel fuel. It was also found that small changes occurred when using either kerosene or jet kerosene as shown in Fig.7.

Table 2 Nasr 592-0501 Diesel Engine Data

Type Four stroke, precombustion chamber, water cooled naturally aspirated diesel engine.

Bore and stroke	125 mm and 140 mm
Capacity	3.44 litres
Compression ratio	22
Max. output	34 HP at 1500 RPM
Max. torque	17 kpm
Injection advance	18 degrees before TDC.

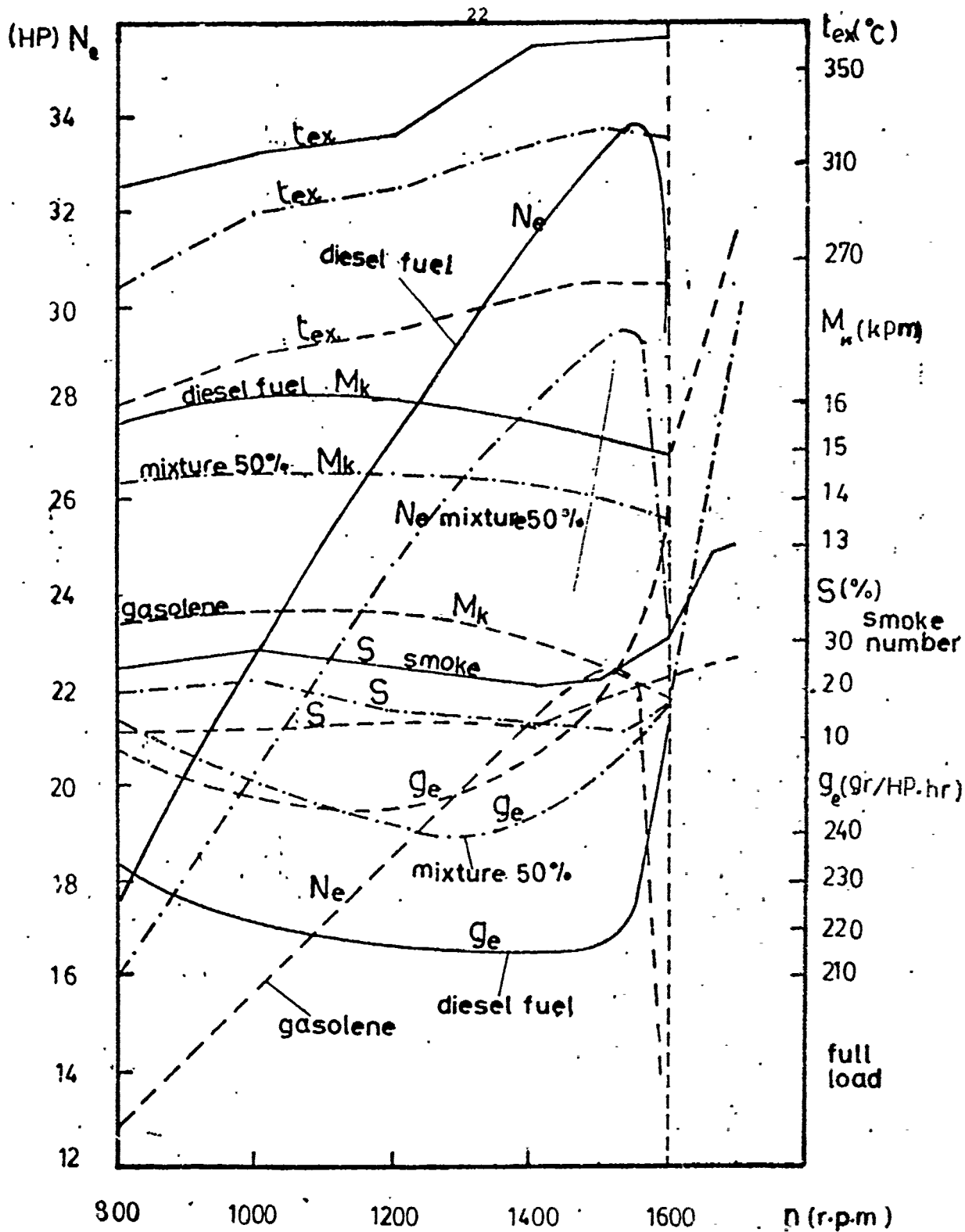


FIG.6 SPEED CHARACTERISTIC OF DIESEL ENGINE NASR WORKING WITH DIESEL FUEL, GASOLENE 70 ON AND MIXTURE OF GASOLENE AND DIESEL FUEL 50 50.

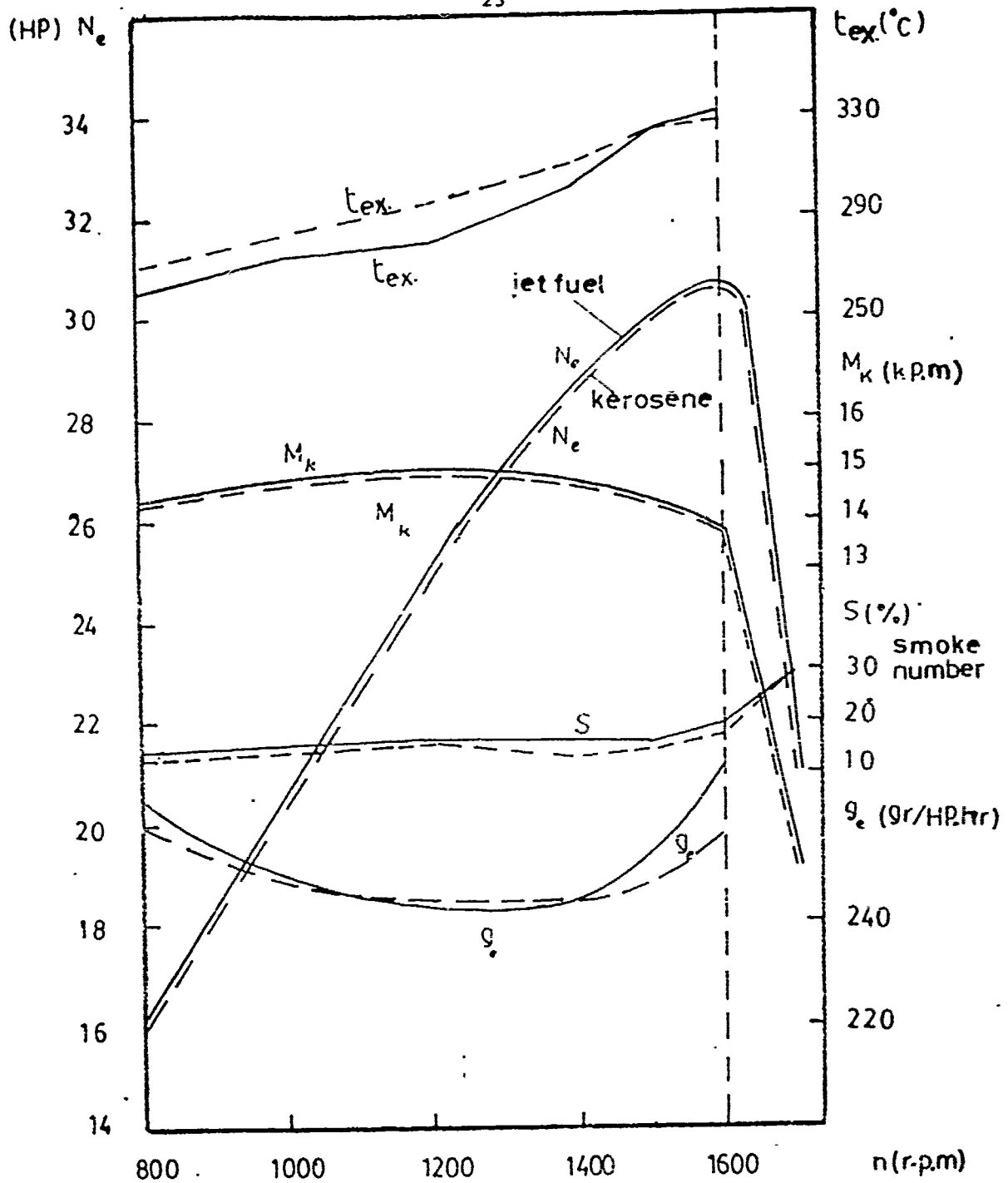


FIG.7 SPEED CHARACTERISTIC OF DIESEL ENGINE NASR WORKING WITH KEROSENE AND JET KEROSENE

CHAPTER 3

OBJECT OF THE PRESENT WORK

It is clear from the previous review that the modified diesel engine, which uses swirl chamber, is suitable to burn smoothly multifuel, and the performance of this engine depends mainly on mixture preparation. Many researches have been carried out to investigate the nature of combustion in swirl chamber diesel engine. Some of these studies have been carried out on experimental basis to determine the effect of swirl chamber shape on the engine performance. These studies were aimed at finding out the swirl chamber dimensions for optimum mixture formation to satisfy minimum fuel consumption, low roughness of combustion, small noise, easy starting and high outputs. Most of these researches led to a rough evaluation of the swirl chamber dimensions. Only few of these researches [1 - 6] have tried to establish a convenient theoretical model of the space-film mixture creation. However, this model is affected by the turbulence motion of air, heat transfer to the chamber and droplets, droplet size distribution, rate of fuel evaporation and the rate of chemical reaction. Moreover, the experimental validity of the model has not been yet done.

The rate of heat release and the roughness of combustion are controlled by the rate of evaporation. The mixture formation inside the swirl chamber depends mainly on the air velocity pattern, the behaviour of the fuel spray either in space or on wall and the mechanism of chemical reaction.

The air velocity pattern was found to depend upon the swirl chamber dimensions and the pressures in the main and swirl chambers. The pattern of air movement inside the swirl chamber was found to be a solid vortex motion at the central part and free vortex motion at the periphery [4]. This has facilitated the establishment of a satisfactory theoretical model for the mean tangential air velocity and medium pressure inside the swirl chamber at various crank angles. However, the determination of the average velocity does not reveal the details of interaction between fuel and air. Over the past decade a considerable effort has been expended on computational procedure with the aid of mathematical models of turbulence for the determination of air velocity in reciprocating engines [7-9]. These prediction procedures are based mainly on the solution of the finite difference of the

governing differential equations for the transport of mass momentum and energy. However, no explicit consideration of the physical properties in swirl chamber has been taken in these attempts. These include the continuous variation of medium pressure and temperature, heat transfer during flow and the shape of the combustion chamber. Moreover, no experimental measurements of the air flow velocity were carried out to carefully compare their values with the predicted one in order to obtain reliable information on the constants of the turbulence model.

The space fuel-air mixing has been studied by several investigators [5,6,1]. ELKOTB et al [2] studied the space fuel-air mixing. Their study was based on the behaviour of a droplet of mean diameter moving at the fuel spray front along the spray axis and subjected to variable heat transfer and drag from the surrounding medium. Thereafter they proposed a somewhat modified model which approximates the fuel spray with a finite number of droplet size groups. They discussed various factors affecting the spray formation and obtained the boundary conditions of the spray at the instant of impingement. Moreover, ELKOTB [1] established a theoretical model for the fuel film motion on the surface of a swirl chamber. But his work is merely theoretical and need be verified experimentally and extended to cover different factors affecting the wall jet.

Data on drop size from various types of fuel injectors and data on single droplet vaporization rate are plentiful. But only limited data have been published on spatial fuel distribution and vaporization rates of sprays. No data have been published on spatial fuel distribution and vaporization rates of mixed fuel with various ratios. Such information is necessary for the development of the spray model in swirl chamber diesel engines.

From the previous discussions, one can conclude that the following parameters are the main factors controlling the space-film mixture formation in swirl chamber diesel engines.

- 1- The operating conditions and their variations with crank angle, swirl chamber geometry, and heat transfer to combustion chamber walls.
- 2- Air velocity pattern inside the swirl chamber and its change with different factors.
- 3- The mechanism of spray formation either in space or on the wall and the factors affecting it.

4- The mechanism of film heating, evaporation and mixing with air to form combustible mixture and the factors controlling these processes.

5- The spatial droplet size distribution of multifuel and factors affecting it.

6- Droplet behaviour and its evaporation for fuel mixtures and factors affecting it.

7- Velocity of chemical reaction and chemical kinetics of fuel mixtures and factors affecting it.

The present project intended to reveal more information about the modelling of multifuel spray formed inside swirl chamber diesel engines. The study of the mentioned parameters are required to satisfy a sufficient accuracy of the spray modelling. Several experimental setups have been built to investigate these factors.

A set up, in which the swirl chamber geometry can be changed, has been built to study the spatial variation of heat transfer in swirl chambers. These experimental results will be used for the validation of the theoretical results.

Another experimental set up consisting of transparent swirl combustion chamber, injection system, high speed photography, hot wire anemometer and the necessary equipment for recording various parameters has been built. This is required for the measuring of air velocity and spray behaviour. A third one, has been built to study the spatial atomization of fuel mixtures using the slide sampling technique.

Other interesting parameters are the droplet behaviour and fuel evaporation. An experimental set up was built to study the former parameter using the flight droplet technique. Another setup was built to measure the latter one using isokinetic sampling probe to pick up the evaporated fuel, burn it and analyse it by infrared analyzers. This can give the rate of fuel evaporation.

Moreover, it is planned to study the chemical kinetics of the multifuel, and a shock tube has been built for this purpose.

In the present report it is intended to present some new results for the heat transfer in swirl combustion chambers. The instantaneous heat flux was determined and a generalized expression has been established for the calculation of the heat transfer to the swirl chamber wall. Moreover, the prediction and measurements of flow velocity in swirl chambers

are presented. Measurements of air velocity are mainly carried out by a hot wire anemometer. Prediction of air velocity are based on the solution of the finite difference form of the governing differential equations for the transport of mass, momentum and energy.

REFERENCES

- 1 Adller, D. and Lyn, W-T. "The evaporation and mixing of liquid Fuel spray in a diesel air swirl" Proc. Instn Mech Engrs 1969-70 vol 184 Pt 3J paper 16.
- 2 ELKOTB, M.M. , ELSABILGI, M.M. and DIAB,R.M. "Spray behaviour inside a swirl chamber of a diesel engine" Ist Mech Power Engg Conference, Cairo 1977 vol.II.
- 3 ELKOTB, M.M. and Rafat, N.M. "Fuel spray Trajectory in diesel Engines" ASME Trans Journal of Engineering for Power, April 1968.
- 4 Viropoff, D.N. and ELKOTB,M.M. "The Computation of the fresh Charge Velocity pattern in an engine cylinder" The Review of Energetic Machines, vol 4, 1968. Moscow.
- 5 Ogasawara, M. and Sami, H. "A Study on the behaviour of a fuel droplet injected into the combustion chamber of a diesel engine SAE Trans., 1967 paper 670468.
- 6 ELKOTB, M.M. RAFAT,N.M. and ELBAHAR, O.M.F. "A Theoretical Investigation of the Behaviour of the pilot fuel spray in the Combustion Chamber of a Dual-Fuel Engine" Ist Annual statistical Conference and Applied Computing Science, Cairo May 1976.
- 7 GOSMAN,A.D. and JOHNS,R.J.R. "Development of a predictive tool for in-cylinder gas motion in engines" SAE" 780315, 1978.
- 8 BONI,A.A., Chapman, M., COOK,J.L. and SCHNEYER,G.P. "Computer simulation of combustion in a stratified charge engine" Proc. sixteenth (Int) symposium on combustion, Aug. 1976.
- 9 RAMOS,J.I.,HUMPHREY, J.A.C. and SIRIGNANO,W.A. "Numerical prediction of Axisymmetric laminar and Turbulent Flows in Motored, Reciprocating Internal Combustion Engines" SAE Trans. paper No. 790356, 1979.
- 10 ELKOTB,M.M. "A prediction model for the fuel film motion over the surface of swirl chambers" Heat and Fluid Flow in Power system components HMT series volume 3 pergamon press, 1979.

CHAPTER 4

SPATIAL VARIATION OF HEAT TRANSFER IN SWIRL COMBUSTION CHAMBERS

ABSTRACT

Experiments were performed to evaluate the instantaneous surface heat transfer in a diesel engine swirl chamber under firing conditions. An experimental set up, in which the swirl chamber facilitated the variation of the relative swirl chamber volume, relative connecting channel area, inclination angle of the connecting channel and fuel pressure had been built. The instantaneous gas temperature was determined using the determined course of heat release, course of pressure in the swirl chamber and the equation of state. Thereafter, the instantaneous heat flux was determined taking into consideration the momentary composition of products and variation of specific heat. Measuring the mean wall temperature together with the previous mentioned results it was possible to determine the instantaneous heat transfer coefficient.

Generalized expression has been established for the calculation of the heat transfer to the swirl chamber wall under variable design and operating conditions.

NOMENCLATURE

a_1-a_6	constants of eqn. (3)
a_s	relative swirl chamber volume, V_s/V_c , dimensionless
A_e	area of tangential port, m^2
A_s	area of swirl chamber surface, m^2
C_d	discharge coefficient, dimensionless
C_{mp}	mean piston speed, m/s
C_p	specific heat of gas at const. pressure, $J/Kg K$
d	diameter, m
D	engine bore diameter, m
Eu	Euler Number, $P_{fo}/\rho C^2$
g	gravity acceleration, m/s^2
h	convective heat transfer coefficient, $J/m^2h K$
K	thermal conductivity coefficient, $J/m h K$
m	mass of fuel, $Kg/cycle$.
M	mass of gas, Kg
n	polytropic index, dimensionless
N	engine speed, RPM
Nu	Nuselt Number, hD/K
P	pressure, bar .

Pr	Prandtl Number, $C_p \mu / K$
Q _R	heat release, KJ
Q _w	heat transfer to wall, KJ
U	specific internal energy of gas, KJ/Kg
R	gas constant, KJ/Kg K
Re	Reynolds Number, $C_{mp} D / \nu$
T	gas temperature, K ₃
v	specific volume, m ³ /Kg
V	volume, m ³
X	dimensionless pressure defined by eqn. (7)
φ	crankangle, degree
φ _C	combustion time in degree crank
ε	engine compression ratio
ρ	density, Kg/m ³
μ	dynamic viscosity, Kg/m hr
λ	equivalence ratio

Subscripts

a	at the beginning of compression stroke
f	fuel
i	inlet to the swirl chamber
m	main chamber
o	initial
s	swirl chamber
t	tangential port
w	wall

INTRODUCTION

The design of internal combustion engines is necessarily becoming more scientific as the standards of performance, economy, and pollution control are increased. One manifestation of this trend is the increasing use of the mathematical simulation as a design and development tool. However, an engine design based on a mathematical model may give some deviated results due to the assumptions in the model. Many authors [1, 2, 3]* noticed that, along with other information, a knowledge of the instantaneous heat transfer to the cylinder surface is necessary to formulate an accurate model of engine processes.

Many authors [4-7] have presented expressions for the surface heat transfer coefficient. The existing formulae are not satisfactory due to the inaccuracy in predicting the general magnitude of the transfer rate. During the compression

* A list of references is given at the end of the chapter.

stroke heat transfer is entirely convective, while during expansion stroke it is convective and radiative. Quite large variations in general magnitude of the convective component of transfer must arise from engine to engine or even from point to point in the same engine because of variation in flow pattern. Theoretical consideration of the nonsteady heat transfer was explored by Pflaum [8] developed by Esler [9] and extended by Oguri [10]. Assumptions were taken in these analyses for the turbulent heat transfer near the surface. In addition correction factor was applied to the black body equation to compensate for variation from black. In compression ignition engines combustion proceeds by means of a diffusion flame created in unhomogeneous fuel-air mixture. Thus, the problem involves radiation from a mixture of gases at high and varying temperature to complicated wall shape. These facts clarified that it is impossible to calculate accurately the radiation transfer during the combustion expansion period and the error obtained, when using correlations based on experimental bases, will be smaller.

Numerous investigations have been carried out to measure the heat transfer rate in an internal combustion engine. Nusselt formula [11] was determined on the basis of heat loss measurements from spherical bombs. Brillling [12] modified Nusselt's expression by introducing a term for the speed. Eichelberg [4] and Pflaum [5] conducted experimental work to measure the instantaneous heat transfer in an operating engine. The heat flux was determined by measuring the wall surface temperature. They used it as a boundary condition for solving the Fourier unsteady heat transfer equation to find the temperature gradient which is a measure of the heat transfer coefficient. Henien [13] reported better agreement with his measurements when replacing mean piston speed by a calculated instantaneous gas velocity. Pischinger [14] noticed that the radiant transfer cannot be neglected. He had made his investigation on several diesel engines with open chamber over a speed range of 350-800 RPM. Using the ratio of maximum charge velocity leaving the squish area to piston speed he was able to correlate the heat fluxes. It was found that the correlation varied proportionally to the ratio of the charge velocity to the piston speed.

Many different expressions have been proposed to correlate the surface heat fluxes in diesel engines. Attention was focused on three correlations upon which most other correlations have been based. The three correlations which are considered in some details are those of Nusselt, Eichelberg, and correlation based on the Reynolds analogy boundary layer theory. The modifications to these three basic forms, which

have been suggested by various authors [6,7] are also considered. It is quite clear that all mentioned formulae fail in one way or another to meet important requirements. Those which are dimensionally nonhomogeneous can hardly be relied upon for extrapolation to conditions different from those of the experiments. Others did not seem to allow correctly either for unsteady conditions nor for swirl chambers.

Therefore, study of the instantaneous surface heat transfer in an indirect injection diesel engine has been carried. An experimental plant has been built to study the effect of various working conditions and geometrical parameters of the swirl chamber on the heat transfer coefficient under firing operation. The cylinder head was prepared with a special combustion chamber which facilitated the variation of the relative swirl chamber volume, the relative connecting channel area, the inclination angle of the connecting channel, and the fuel pressure. Generalized equation is established for the calculation of the instantaneous heat transfer to swirl combustion chamber.

EXPERIMENTAL INVESTIGATION

In view of the requirement for a detailed understanding of the effect of various factors on heat transfer in swirl combustion chambers, an experimental set up has been built. The engine was a 4-stroke, single cylinder, swirl chamber diesel engine with a 70 mm bore, 57 mm stroke and a compression ratio 17. The engine was coupled to an electric dynamometer and instrumented for obtaining performance data such as speed, power and consumption of air and fuel. The general layout of the experimental plant is shown in Fig. 8. The swirl chamber was constructed in the form of a sphere of two parts. The two parts are fixed to the cylinder head by two stud bolts on the top corner of the cylinder. The swirl chamber arrangement is shown in Fig. 9. The lower part of the chamber can be changed to allow for the variation of the inclination angle and area of the tangential port. The swirl chamber can be changed also for the variation of the swirl chamber volume without changing the compression ratio. The swirl chamber was supplied by the fuel from the top by a pintle type injector with a single hole of diameter 1 mm and injection angle 90 degree.

For measuring the mean surface temperature six surface thermocouples constructed from chromel-Alumel were immersed deeply near to the surface in six locations in the periphery

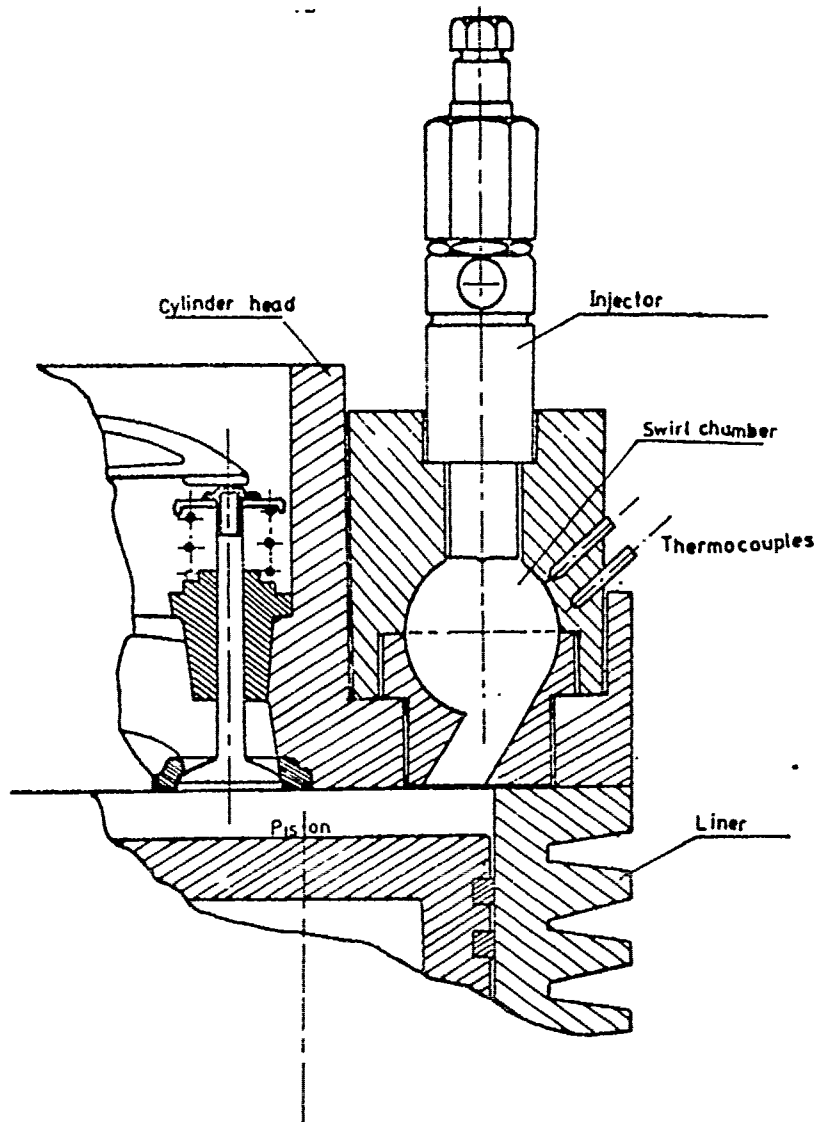


FIG.9

SCHEMATIC DRAWING OF THE SWIRL CHAMBER FOR HEAT TRANSFER STUDY.

of the swirl combustion chamber. The fixation of thermocouples was satisfied such that the disturbance to the heat transfer pattern was kept to a minimum and the thermocouple junction temperature was considered to be the true surface temperature. A selector switch and a potentiometer were used to measure the time averaged value of the inside surface temperature of the chamber wall.

The rapid variation of gas pressure inside the combustion chamber together with the crankangle were picked by a highly sensitive transducer of sensitivity 10.95×10^{-12} C/bar and natural frequency 100 KHZ and an external X-generator consequently. The display of the gas pressure was synchronized with the crankshaft by a disc displaying the signal of the top dead centre. A strain gauge system and inductive transducer were used for recording fuel line pressure and needle lift facilitating the calculation of the instantaneous rate of fuel injection. A sample of the results is shown in Fig.10. A precise fuel flow meter was installed between the tank and the injector to measure the rate of fuel delivered to the engine. This was used to facilitate the choice of the suitable discharge coefficient of the injector.

The data recorded during an engine run included combustion chamber pressure, crankangle, top dead centre and six surface temperatures. Because of the cycle to cycle variations in data recorded and hence in surface heat flux, it was required to examine a large quantity of data if meaningful and significant results were to be obtained. Thus, a high speed multichannel data recording and processing system was developed. The output from each transducer was magnified and recorded by an 8-channel magnetic tape recorder. A calibration signal was recorded at the start of recording. Thereafter the analog signal representing chamber pressure was displayed back from the tape recorder at a lower speed to the analog-digital converter and digitized at every crank for 50 cycles. The output signals of the six thermocouples, fuel line pressure and needle lift were also treated in the same way. The output of the 50 cycles was then processed and the average cycle pressure variation and surface temperature were determined and recorded onto magnetic tape in digital form for subsequent processing on digital computer to determine the surface heat flux. This technique facilitated also the attenuation of the random noise introduced by the electronic components.

The aim of the experimental investigation was the study of the effect of volume, throat diameter, throat angle of the swirl combustion chamber on heat transfer rate. Thus, the

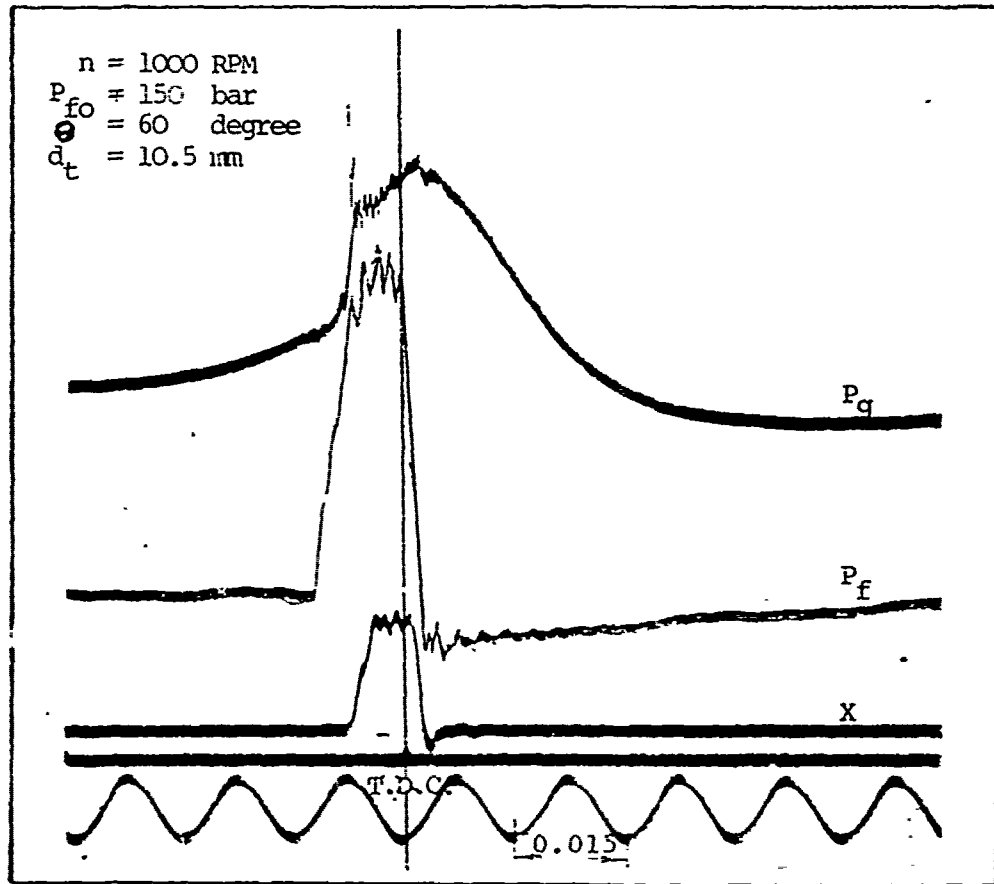


Fig.(10) The courses of swirl chamber gas pressure, fuel pressure, needle lift & the location of TDC in relation with time.

essential factors were varied as follows :

- 1- Diameter of the swirl chamber ranging between 21.5 mm and 26 mm satisfying swirl chamber volume ratios ranging between 0.024 to 0.042.
- 2- Throat diameter of tangential port ranging between 7 mm to 10.5 mm satisfying throat area ratios ranging between 0.1 to 0.15.
- 3- Throat angle of swirl chamber ranging between 45 and 90 degree satisfying various inlet moment of momentum.
- 4- Engine speed ranging between 1500 and 2500 RPM.
- 5- Injection pressure ranging between 85 and 140 bar.
- 6- Engine load varying between 1/4 and full load.

One engine operating condition, which is given in Table 1, was defined as the standard operating condition. Any variable whose value is not specified may be assumed to be the standard value.

Table 1 Standard operating conditions

Compression ratio	17
Engine speed	2000 + 20 RPM.
Fuel injection advance	24 + 1 degree CA BTDC
Inlet temperature and pressure	300 K, 1 bar
Inlet valve opens and closes	704 degree CA and 216 degree CA.
Exhaust valve opens and closes	496 degree CA and 8deg.CA
Fuel	light diesel fuel.
Fuel opening pressure	110 bar.
Throat area ratio	0.12
Throat angle	60 degree.
Swirl chamber volume ratio	0.024.

HEAT TRANSFER MODEL FOR A SWIRL CHAMBER DIESEL ENGINE

The theory used here simply computes the heat flux from pressure time data. The mathematical model and calculation procedure is thus a refined model of obtaining data for further correlation studies.

The model assumes thermodynamic equilibrium at each instant. Thus it is assumed that the entire cylinder contains homogeneous mixture of air and combustion products at each instant.

Phenomena such as fuel vaporization, mixing, temperature gradients, and so are thus ignored. The instantaneous equilibrium composition are considered in the model. With these assumptions the energy equation during the compression stroke, where the air flows from the main combustion chamber to the swirl chamber, becomes ;

$$\frac{dQ_R}{d\phi} - \frac{dQ_W}{d\phi} = - \frac{dM_i}{d\phi} (U_m + R T_m) + M_s \frac{\delta U_s}{\delta \lambda} \frac{d\lambda}{d\phi} + \frac{\delta U_s}{\delta T} \frac{dT_s}{d\phi} + U_s \frac{dM_s}{d\phi} \quad (1)$$

and during the expansion stroke becomes ;

$$\frac{dQ_R}{d\phi} - \frac{dQ_W}{d\phi} = - \frac{dM_s}{d\phi} (U_s + R T_s) + M_s \frac{\delta U_s}{\delta \lambda} \frac{d\lambda}{d\phi} + \frac{\delta U_s}{\delta T} \frac{dT_s}{d\phi} + U_s \frac{dM_s}{d\phi} \quad (2)$$

Before fuel burning the quantity of heat released Q_R and the term $(\delta U_s / \delta \lambda) (d\lambda / d\phi)$ are equal to zero. The internal energy of the products of combustion of fuel and air were calculated at the equilibrium state using the data from JANAF tables [14]. The fuel is assumed to take the form $C_{16}H_{34}$ and complete combustion is assumed due to presence of excess air in diesel engines. The effect of dissociation is largest at low pressures, high temperatures and excess air factor near unity. However, the equilibrium composition was calculated from the equation of combustion for various temperatures. The average specific heat and gas constant of the constituents were calculated and were then fit as a function of T P to achieve a great save of computer time. The final equation for the internal energy and the gas constant were thus found to be given by ;

$$U = a_1 + a_2 (\lambda - 1) - a_3 T + a_4 T^2 + a_5 T^3 + a_6 (\lambda - 1) T$$

for $\lambda < 1.6$ and $T > 1333$ degree K.

$$U_1 = U + 14.2029 (T - 1388.89)^{4.5371} |1 - 10(\lambda - 1)| / P^{0.46024}$$

where,

Const.	a_1	a_2	a_3	a_4	a_6
$\lambda > 1.6$ $T < 1333K$	- 2888.78	595.25	0.668454	2.713×10^{-4}	$- 7.40325 \times 10^{-8}$
$\lambda > 1.6$ $T > 1333K$	- 3466.2	903.84	0.65898	$- 3.8 \times 10^{-4}$	8.2329×10^{-8}

$$R = 0.22751 + 0.063438\lambda - 3.33005 \times 10^{-3} \lambda^2 \quad (4)$$

The partial derivatives can be written explicitly in terms of temperature and equivalence ratio. The time derivative of the equation of state gives an expression for $dT_s/d\phi$ in the following form :

$$dT_s/d\phi = T_s \left\{ \frac{dP_s/d\phi}{P_s} - \frac{dM_s/d\phi}{M_s} - \frac{dR/d\phi}{R_s} \right\} \quad (5)$$

This equation is used to eliminate that quantity from the energy equations 1 and 2.

The inlet mass to the swirl chamber was calculated from the model suggested by ELKOTB [15], in which a relation of the instantaneous pressures inside the main and swirl chambers is derived in the following form :

$$\frac{dX}{d\phi} = \frac{X}{v/v_s} \frac{d(v/v_s)}{d\phi} + \frac{30 C_d A_e \sqrt{P_o v_o}}{\pi N V_s} \sqrt{2g \frac{n}{n-1} \left(\frac{1}{v/v_s}\right) (\epsilon/a_s)^{\frac{n-1}{2}}} \cdot (X+v/v_s)^{\frac{3-n}{2}} - \sqrt{1-X^{n-1}} \quad (6)$$

where,

$$X = (P_s/P)^{1/n} \quad (7)$$

$$P = \left[(\epsilon/a_s) / (X + v/v_s) \right]^n \quad (8)$$

The solution of this differential equation gives the instantaneous value of the dimensionless swirl chamber pressure. The swirl chamber pressure values are calculated from a smoothed pressure-crankangle using a second degree Lagrangian interpolation formula. This is required to check the value of the discharge coefficient chosen in eqn 6. The rate of mass flow to the swirl chamber can thus be written in the following form :

$$\frac{dM_i}{d\phi} = C_d A_e \sqrt{2g \frac{n}{n-1}} T_a (P/P_a)^{\frac{n-1}{n}} \sqrt{1 - (P_s/P)^{\frac{n-1}{n}}}$$

This is equal to the rate of increase or decrease of the mass in both chambers.

Before combustion proceeds the quantity of burned fuel is equal to zero and the equivalence ratio in both chambers is infinity. After ignition the quantity of fuel increases and the equivalence ratio in the swirl chamber based on the burned fuel decreases. An increase of pressure occurs causing a

flow of fuel-air mixture and exhaust gases from the swirl chamber to the main chamber. Therefore, the equivalence ratio in the main chamber starts to decrease. The quantity of burned fraction at any instance from the beginning of combustion was estimated from the equation proposed by Setki [16] as follows :

$$m_{f\phi}/m_f = 1 - |\exp - 6.9 (\phi/\phi_c)^{m+1}|$$

where,

$$m = (3.2 / \log \phi_c) - 1$$

The instantaneous injected fuel quantity was determined experimentally and therefore the quantity of unburned fuel flowing to the main chamber can be determined. Thus, the quantity of heat released inside the swirl chamber is calculated as follows :

$$d Q_R/d \phi = c.v (d m_f/d \phi)$$

For small interval of crankangle the equivalence ratio at the end of the interval is calculated from the calculated equivalence ratio at the beginning of the interval and the rate of fuel burning during the interval $d \phi$. For swirl chamber the quantity of burned fuel at the end of interval is equal to the quantity of burned fuel at the beginning plus the burned fuel during the interval $d \phi$ minus the quantity of burned fuel flow to the main chamber. Thus, the rate of change of the equivalence ratio can be determined.

RESULTS OF THE HEAT TRANSFER CALCULATIONS

Calculations of instantaneous heat transfer coefficient have been carried out using pressure crankangle data. The surface temperature of the swirl chamber must be estimated from experimental data. Therefore, the experimental results obtained in the present work consists mainly of measurement of mean wall temperature, measurement of pressure time diagram and measurement of fuel delivery law. These data were obtained from a swirl chamber air cooled, single cylinder research engine at various operating conditions (engine speed, load and fuel opening pressure) and various geometrical dimensions of the swirl Chamber.

The effect of swirl chamber volume, throat area of the tangential port, inclination angle of the tangential port and

fuel opening pressures on the mean surface temperature was studied. For each chamber the surface temperatures at four locations were measured at various speeds while the factors were kept constants at the standard values given in Table 1. The mean wall temperature was calculated from the arithmetic mean value of the four measured temperatures. The results at various engine speeds and fuel load are given in Figs. (11) to (14). One notices from Fig. (11) that the mean wall temperature decreases with the increase of engine speed, but the rate of decrease is relatively great in swirl chambers with greater diameters than with small diameters. It is clear also that the mean wall temperature increases when the diameter of the swirl chamber increases as the heat transfer to the walls increases with the increase of the surface area. The moment of momentum increases also with the increase of diameter and consequently the gas velocities inside the chamber increases giving an increase to the heat transfer to the walls.

One notices also from Fig. (12) that the mean wall temperature increases when the throat area ratio increases or decreases than 0.1 since the cooled air at the entrance of the port is small in this case and the moment of momentum increases with the increase of the throat diameter. The variation of the inclination angle of the tangential port showed that the mean wall temperature is greater in swirl chamber with throat inclination of 45 and 90 degree than of 60 degree, as shown in Fig. (13) due to the presence of cooled air at the entrance of the tangential channel. The variation of the fuel opening pressure shows an increase of the mean wall temperature with the increase or decrease of the fuel opening pressure than 110 bar, as shown in Fig. (14). This is believed to be due to improvement of fuel air mixing at this fuel opening pressure. Similar results were obtained at various loads.

Calculations of heat release in these swirl chambers have been carried out. Samples of the results for the rate of heat release are shown in Fig. (15). The first peak in the heat release corresponds to the period of rapid pressure rise and lasts for only about 2 degrees C.A. The second stage corresponds to the period of gradually decreasing rate of heat release and lasts about 13 degrees C.A. This is the main heat release period. Normally about 80 percent of the total heat is released in these two periods. The third period corresponds to the tail of the rate of heat release diagram in which a small rate of heat release occurs.

The surface heat flux and the heat transfer coefficient have been calculated at full load and at engine speed 2000 RPM using the previous calculated heat release, mass transfer from

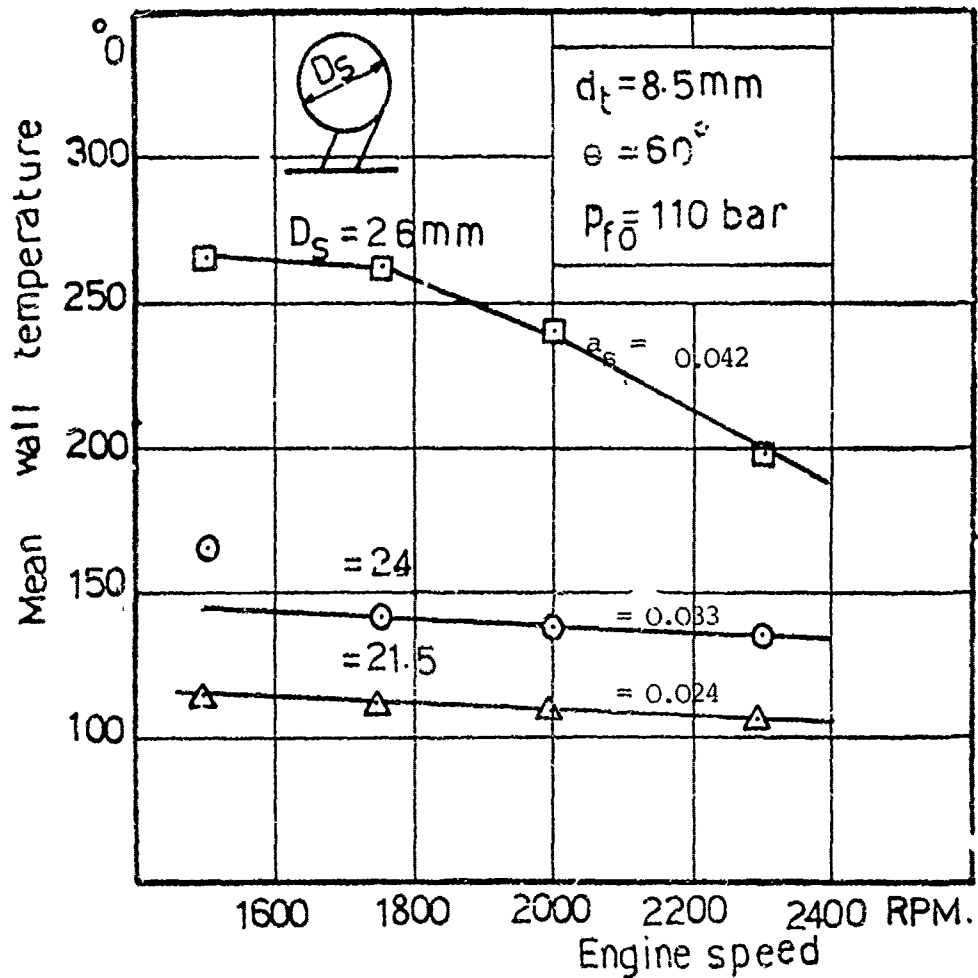
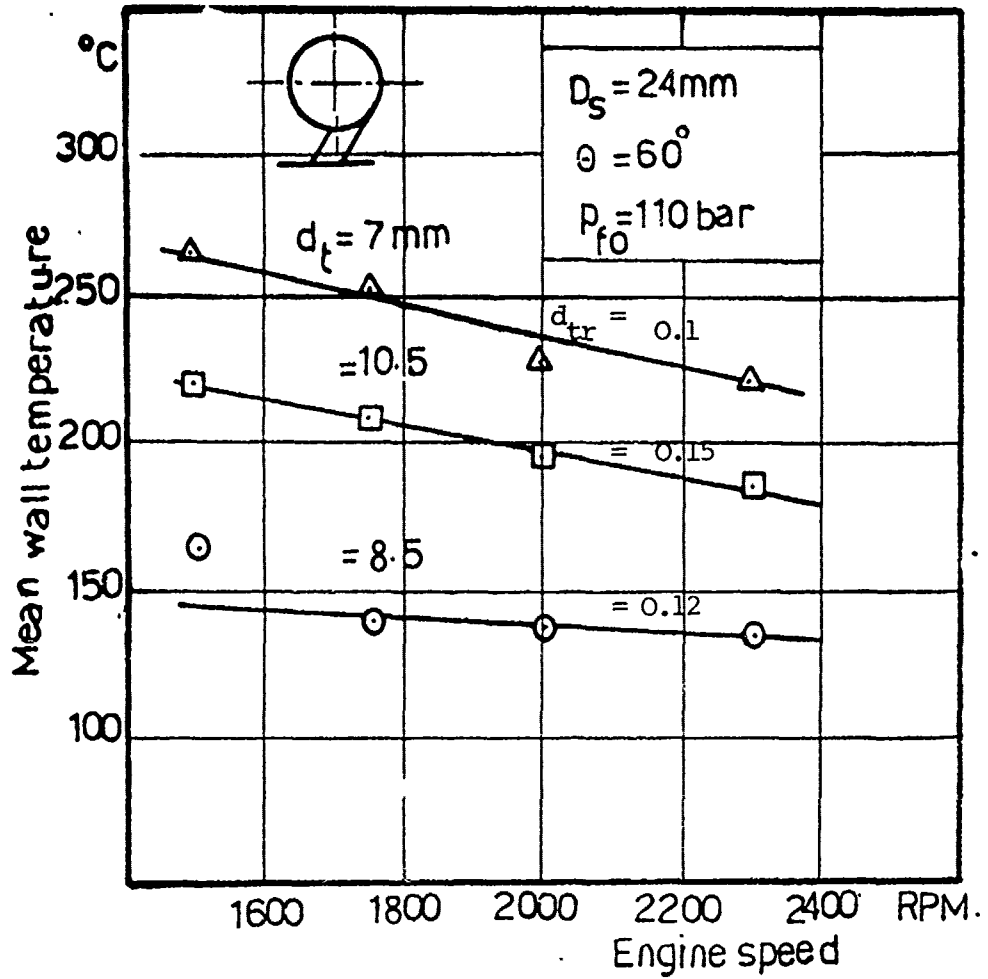
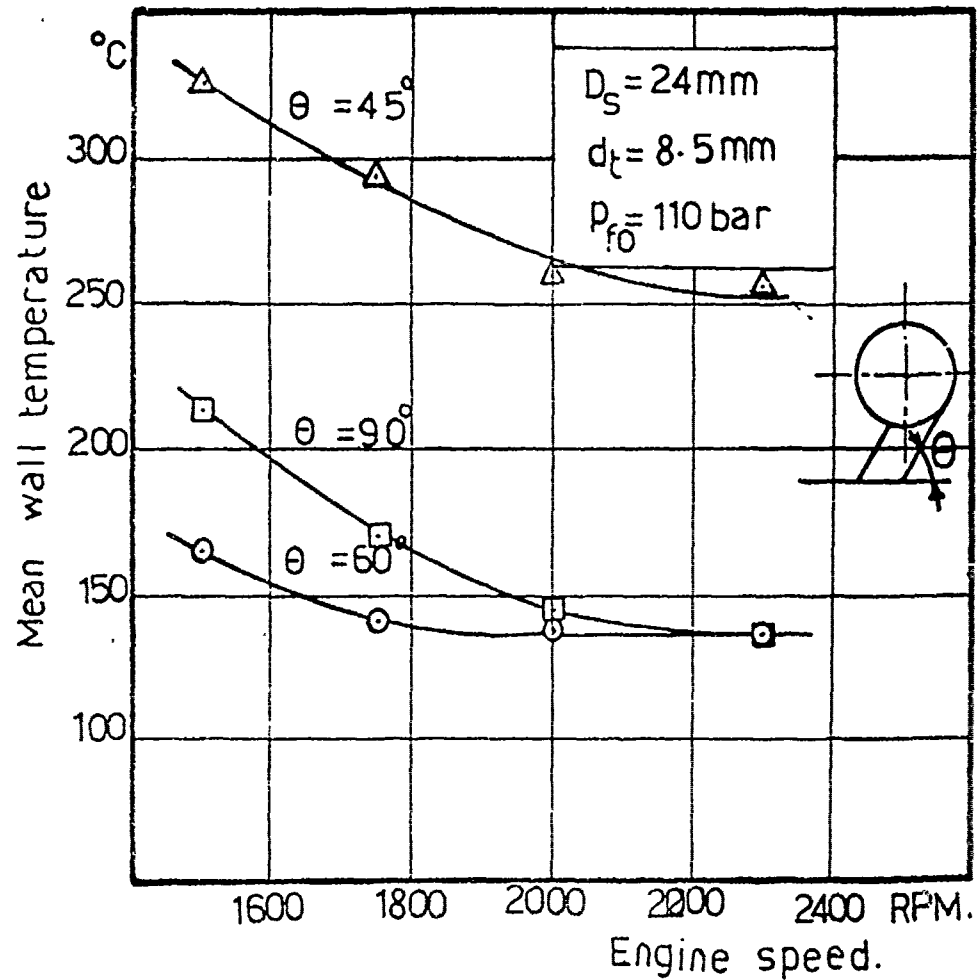


Fig. II Relation between mean wall temperature and engine speed for different swirl chamber volume ratios at full load.



Fig(12.) Relation between mean wall temperature and engine speed for different throat diameter of the tangential channel at full load.



Fig(13)Relation between mean wall temperature and engine speed for different inclination angles of the tangential channel at full load.

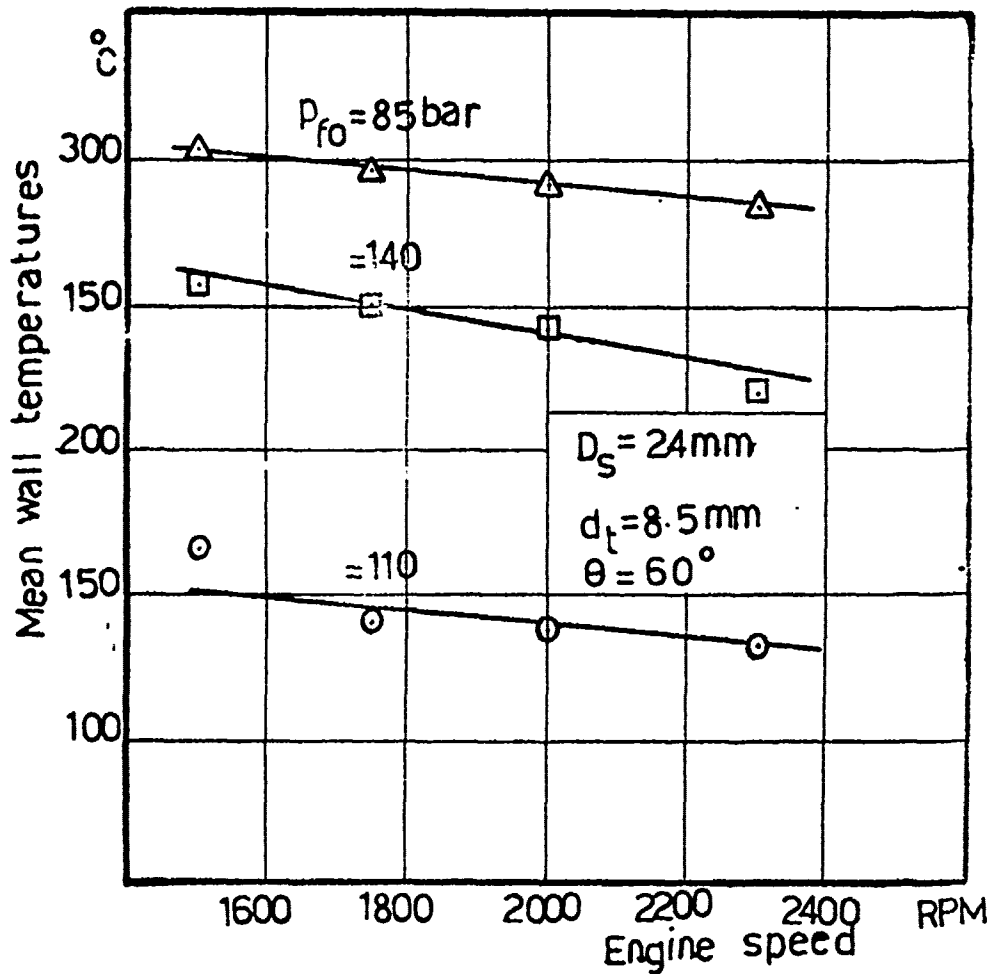


Fig. 14 Relation between mean wall temperature and engine speed for different opening pressures of the injector at full load.

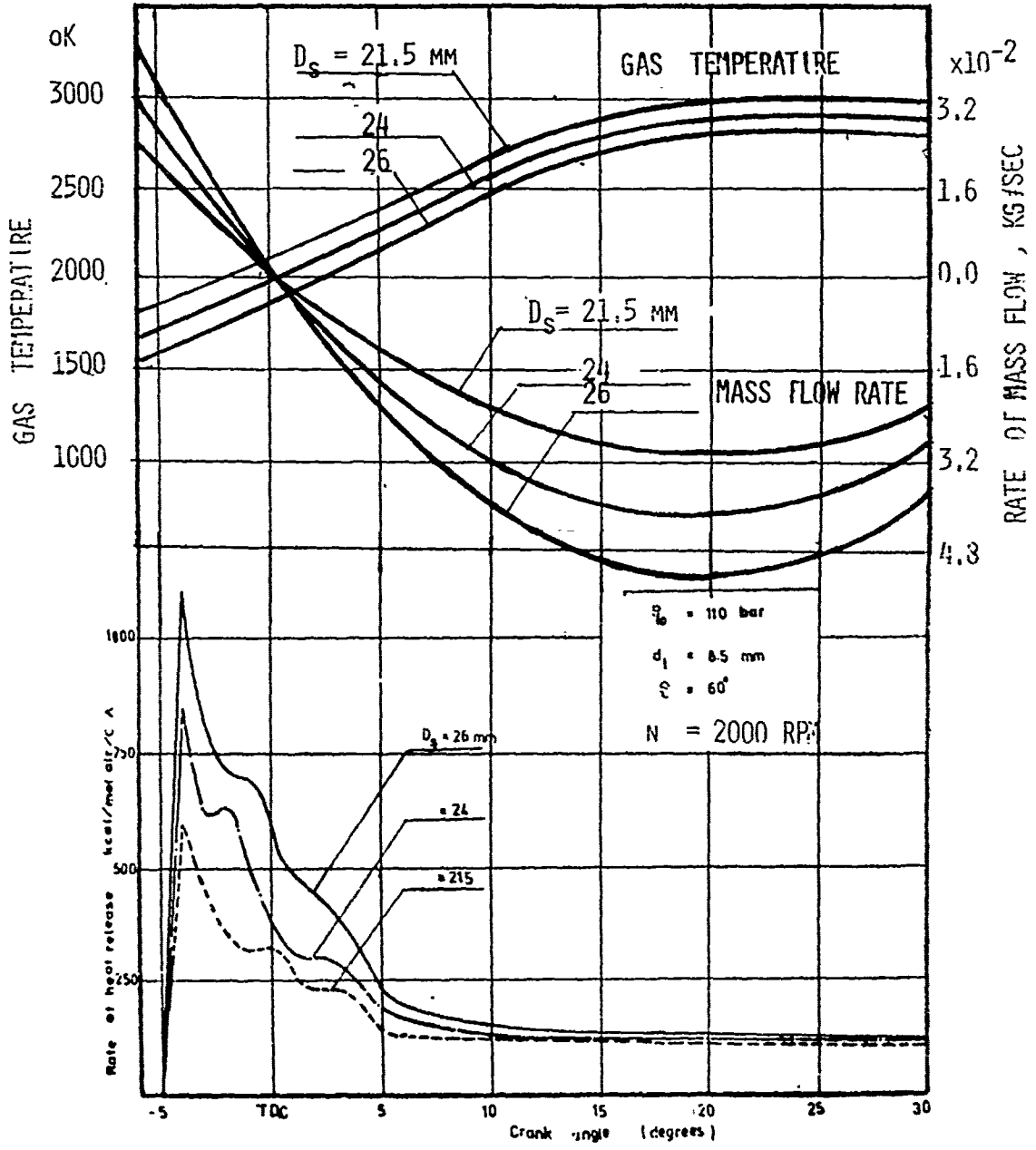


Fig. 1b Effect of varying swirl chamber volume on rate of heat release

the swirl chamber to the main chamber, Fig. (15), and the calculated gas temperature. The instantaneous gas temperature has been calculated using the equation of state for which the instantaneous gas constituents with dissociation were calculated. The calculated heat flux and the heat transfer coefficient for various swirl chamber diameters are shown in Fig. (16). The surface heat flux increases firstly reaching maximum value at the T.D.C. and decreases again. The values of the surface heat flux increases with the increase of the swirl chamber diameter. The moment of maximum heat flux is not affected with the change of chamber volume. The heat transfer coefficient increases also similarly, as the surface heat flux, with the increase of chamber volume and the maximum value of the heat transfer coefficient is nearly at the T.D.C.

The effect of the throat diameter and the inclination angle of the tangential port on the surface heat flux and the heat transfer coefficient have been studied and the results are illustrated in Figs. (17) and (18). The influence of the throat diameter and the inclination angle is not great compared to the effect of the chamber volume. Minimum value of heat transfer coefficient is obtained when the throat diameter was 8.5 mm and the inclination angle 60 degrees. The location of the maximum value is not affected with the change of the throat diameter and the inclination angle. The effect of fuel opening pressure has been also studied and the results are illustrated in Fig. (19). It was found that the heat transfer coefficient has greater values with fuel opening pressure of 85 bar and smaller values with fuel opening pressure of 110 bar. This means that when the fuel opening pressure increases or decreases than 110 bar the quantity of fuel burned in the swirl chamber increases.

CORRELATION AND COMPARISON OF HEAT TRANSFER COEFFICIENT

It is clear from the previous discussion that the heat transfer process is a very complex phenomenon and the early empirical relations were unsatisfactory due to their suitability to specified engine. An obvious solution to this complicated problem is to derive the dimensionless groups assuming steady state system at any instant. The variables affecting the heat transfer process in this case are as follows ;

$$h = f(D, d_s, d_t, C_{mp}, C_p, \mu, K, P_{fo})$$

The application of dimensionless analysis reduces the variables to the following dimensionless groups :

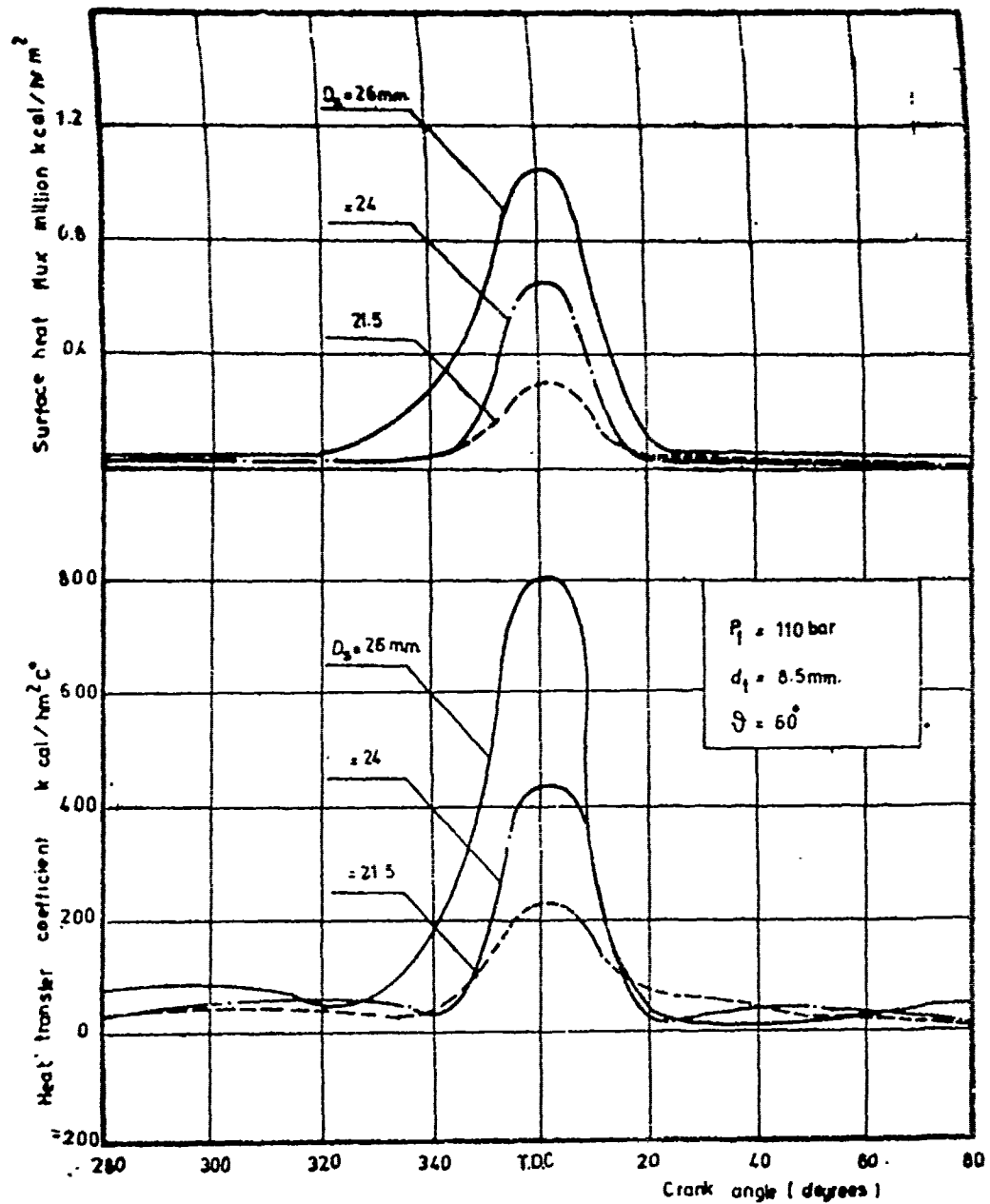


Fig (16) Effect of varying swirl chamber volume on heat transfer coefficient and surface heat flux.

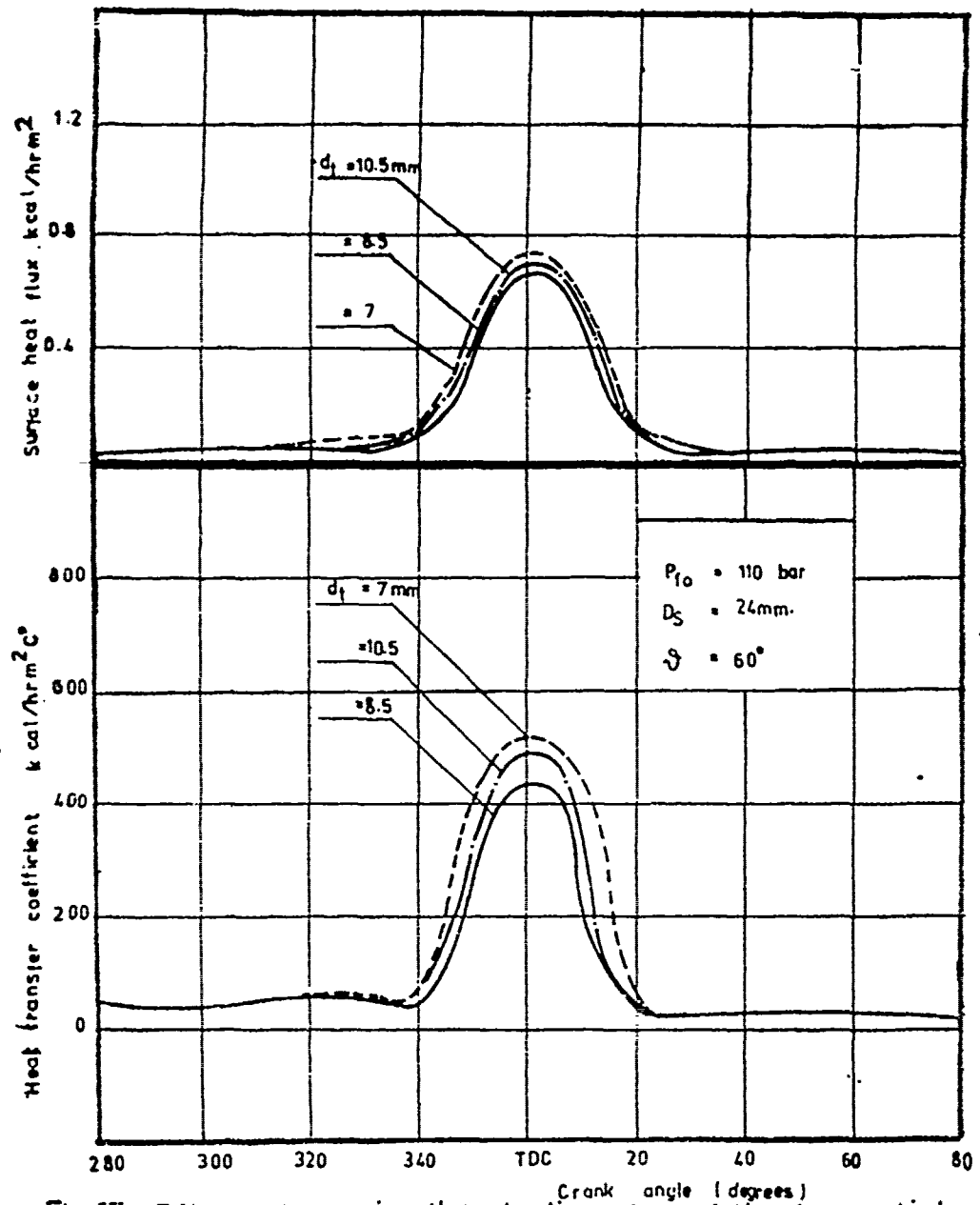


Fig.17) Effect of varying throat diameter of the tangential channel on heat transfer coefficient and surface heat flux.

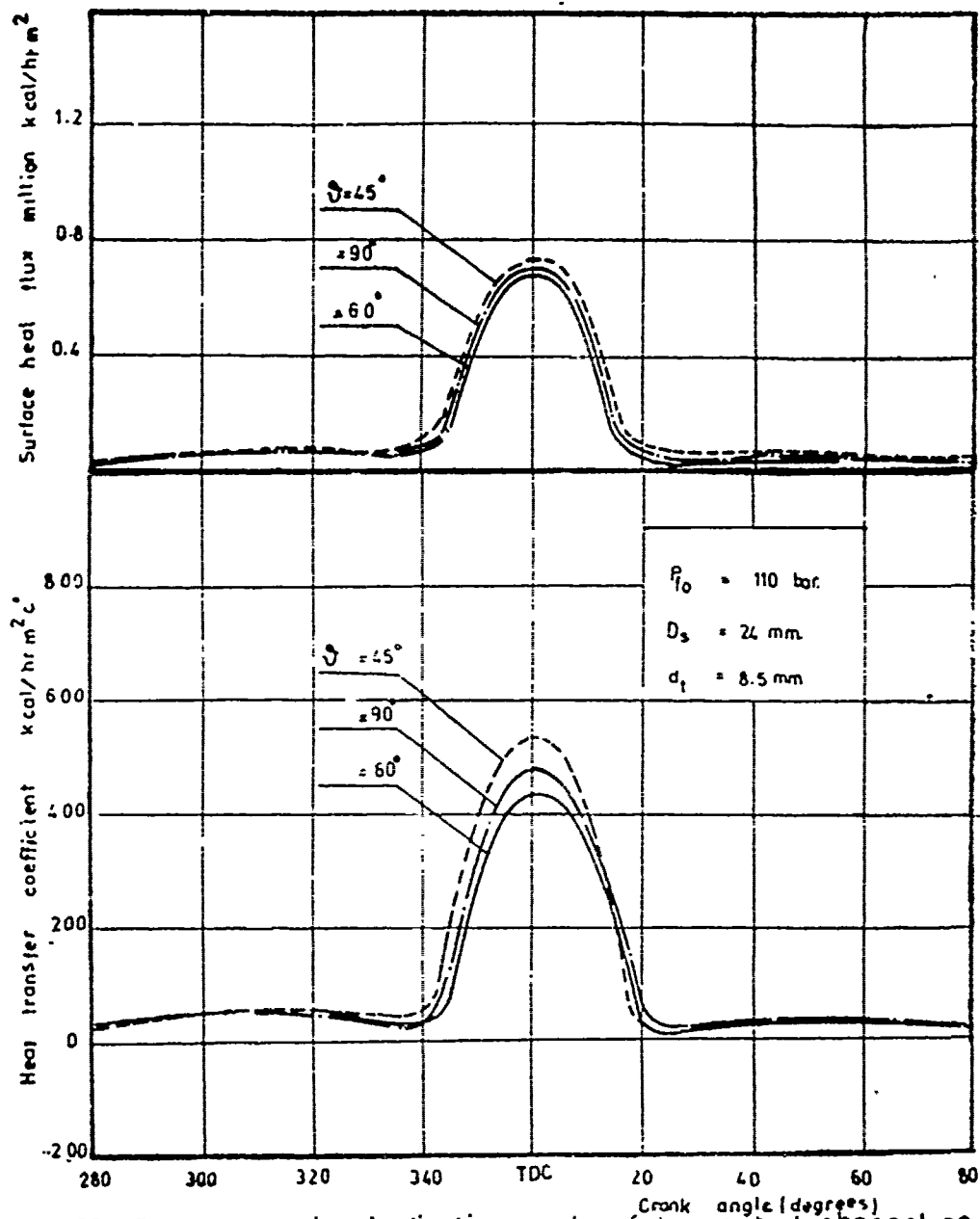


Fig. 18 Effect of varying inclination angle of tangential channel on heat transfer coefficient and surface heat flux.

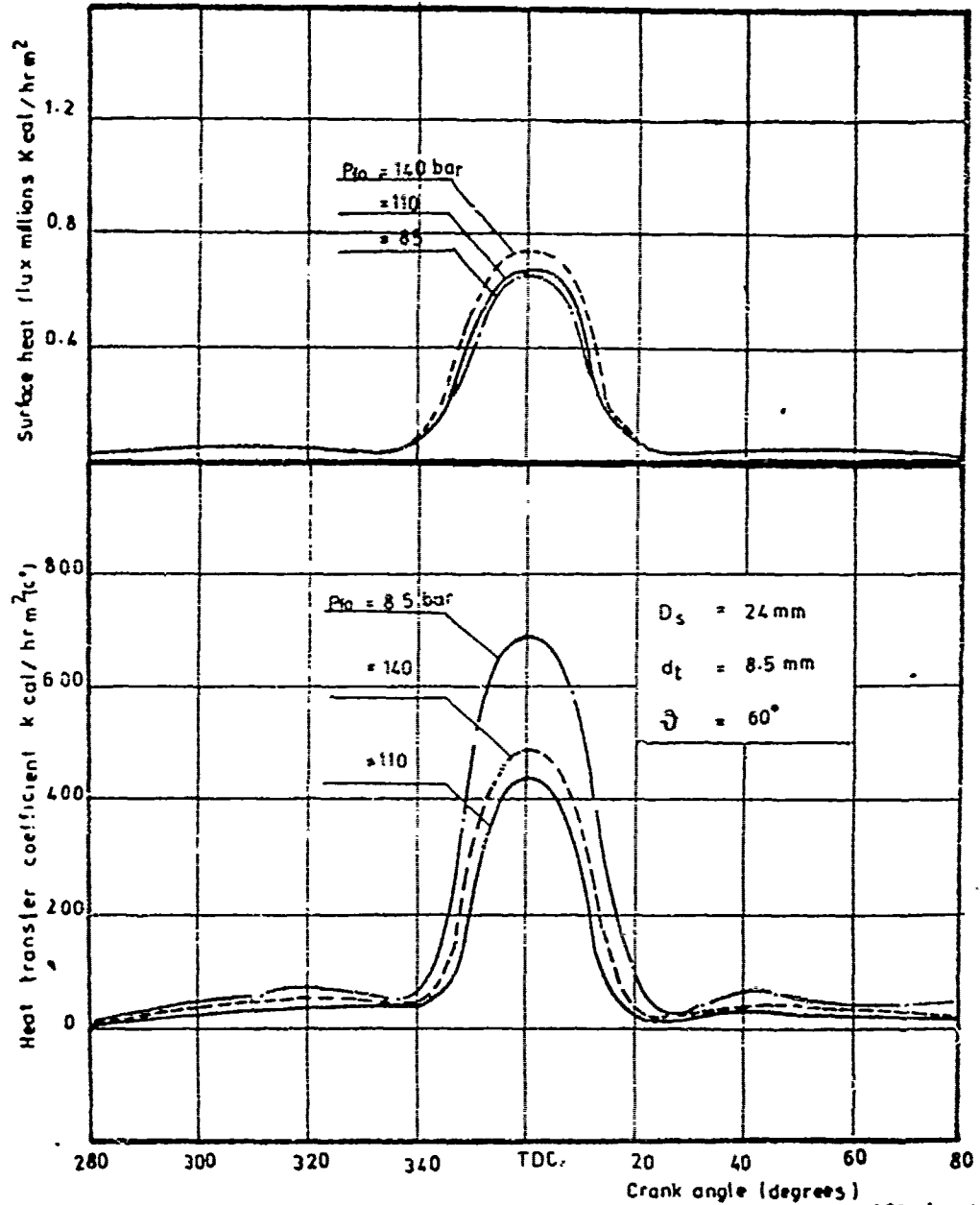
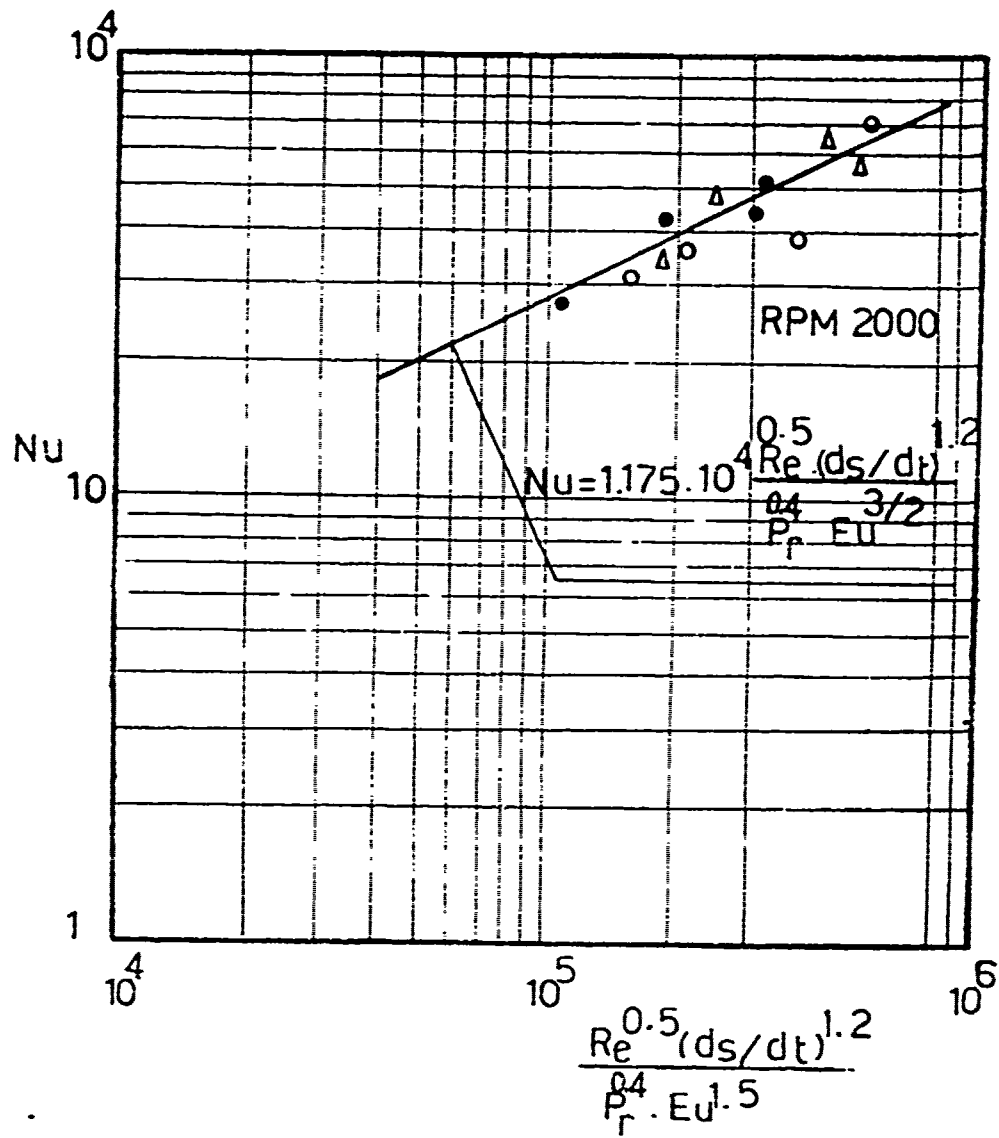
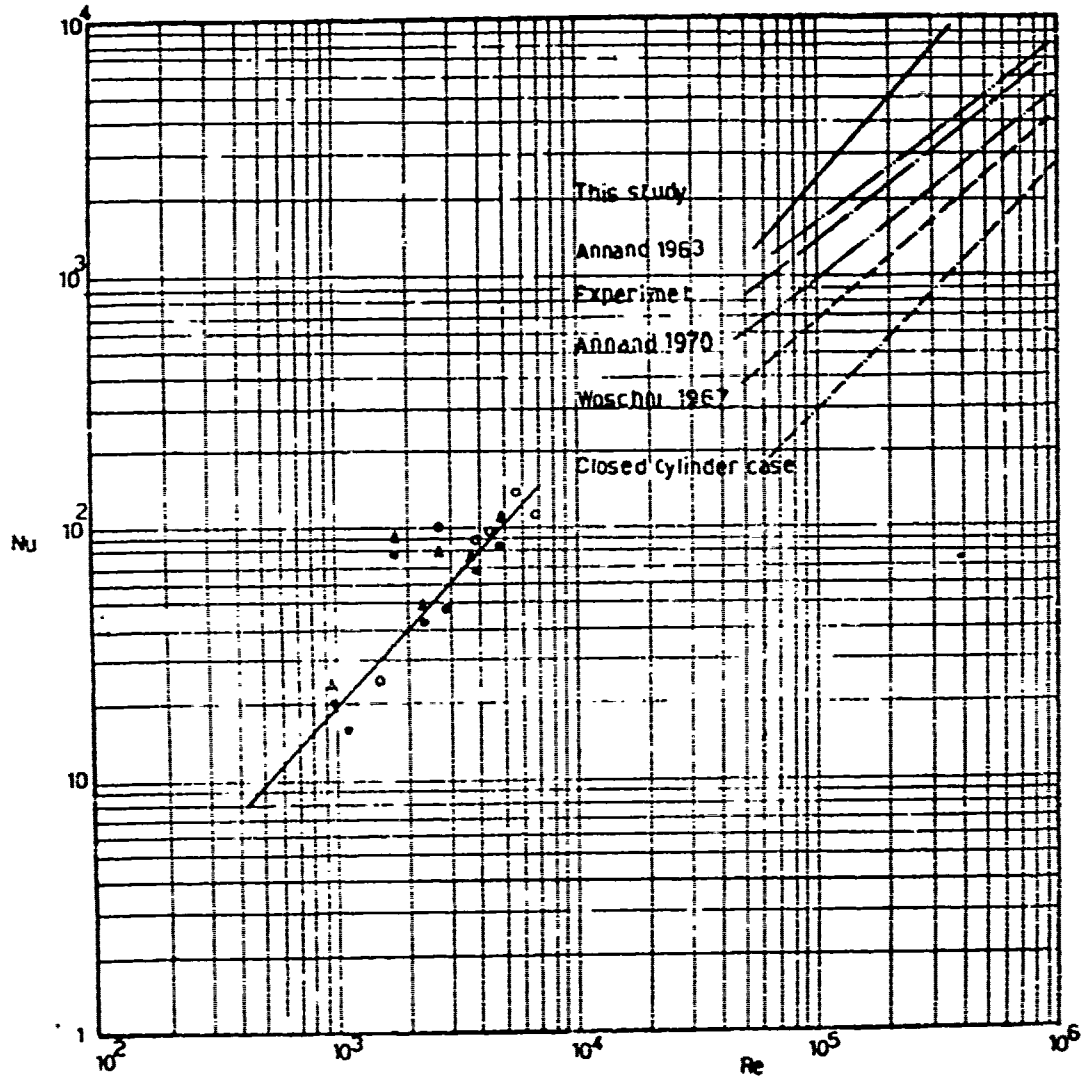


Fig 19 Effect of varying pressure on heat transfer coefficient and heat flux.



Fig(20)Relation between Nusselt Number
and $\frac{Re^{0.5} (ds/dt)^{1.2}}{Pr^4 Eu^{1.5}}$



$$\frac{hD}{K} = f\left(\frac{\rho C_{mp} D}{\mu}, \frac{C_p \mu}{K}, \frac{P_{fo}}{\rho C_{mp}^2}, \frac{d_s}{d_t}\right)$$

and the equation of the heat transfer becomes :

$$Nu = A Re^a Pr^b Eu^c (d_s/d_t)^e$$

Using the experimental results the indices of the dimensionless quantities were determined by plotting the Nusselt number versus one of these quantities. The indices that fit the experimental values by a smooth curve are the required values for the generalized equation. Thereafter, plotting the Nusselt number versus the dimensionless quantities raised to the obtained indices as shown in Fig.(20), the constant of the generalized relation was obtained. The generalized relation has been found in the following form :

$$Nu = 1.175 \times 10^{-4} Re^{0.5} Pr^{-0.4} Eu^{-1.5} (d_s/d_t)^{1.2}$$

Comparing the results of this work with other previous studies such as Woschni, Annad (1970), Annad (1963) and it is clear from Fig.(21) that Nusselt number in this study for the same Reynolds number is greater than all other values. This was expected as the velocity and turbulence of the mixture in the swirl chamber is more than in the open chamber.

REFERENCES

- [1] ELKOTB, M.M. and ELGONEIMY, M.N. "The Apparent Heat Release of Burning Multi-Fuel in Open Combustion Chambers" Proc. of Vth Int. Symposium on Combustion Processes, Krakow Sep. 1977, Poland.
- [2] CHONG, M.S., MILKINS, E.E. and WATSON, H.C. "The prediction of Heat and Mass Transfer During Compression and Expansion in I.C. Engines" SAE Trans. 760761, 1976.
- [3] Gosman, A.D. et al "Axisymmetric Flow in a Motored Reciprocating Engine" Proc. of Inst. of Mech. Engineers, vol. 192, No. 11, pp. 213-223, 1978.
- [4] EIHELBERG, G. "Some New Investigation in Old Combustion Engine Problem" Engineering, V. H8, 1935.
- [5] PFLAUM, W. "Warmeübergang bei Diesel Maschinen mit und Ohne Aufladung" MTZ Vol. 22, No. 3 March 1961; Translated in The Engineers Digest, Vol. 22, No.7, 1971.
- [6] ANNAND, W.J.D. "Heat Transfer in the Cylinders of Reciprocating Internal Combustion Engines" Proc. Inst. Mech. Engrs Vol. 177, No. 36, 1963, P.973.

- [7] WOSCHNI "A Universally Applicable Equation for the Instantaneous Heat Transfer Coefficient in the Internal Combustion Engine" SAE paper No. 670931, 1967.
- [8] PFLAUM, W. "Heat Transfer in Internal Combustion Engines" Presented at Ia Conferenza Internazionale di Termotecnica, Milan, Nov. 1962.
- [9] FLSEER, K. "Der Intationaire Wameubergang in Dieselmotoren" Mitt. Inst. Thermodyn. No. 15 Zurich, 1954.
- [10] OGURI "Theory of Heat Transfer in the Working Gases of Internal Combustion Engines" Bull. Sec. Mech. Engrs, 3, 370.
- [11] NUSSELT, W. "Der Wameubergang in der Verbrennungskraftmaschine" VDI Forschungshaft, No. 264, 1923.
- [12] BRILLING "Correlation of Cooling Data from an Air Cooled Cylinder and Several Multicylinder Engines" Bull. of Scientific Aviatechnical Inst. "NATU" Vol.31, 1927.
- [13] HENEIN, N.A. "Instantaneous Heat Transfer Rates and Coefficients Between the Gas and Combustion Chamber of a Diesel Engine" Paper 969B Presented at SAE Meeting, Detroit, Jan. 1965.
- [14] JANAF Interim Thermodynamic Data Tables "Dow Chemical Corporation, Midland, Mich. 1960.
- [15] ELKOTB, M.M. et al "Theoretical Investigation of Velocity Air Pattern Inside the Swirl Chamber" Bull. of Faculty of Engng, Cairo University, Paper 17, 1976.
- [16] SITKEI, G. Kraftstoffaufbereitung und Verbrennung Bei Dieselmotoren. Berlin 1964 Springer Verlag.

CHAPTER 5

PREDICTION AND MEASUREMENT OF FLOW AND HEAT TRANSFER IN MOTORED DIESEL ENGINES SWIRL CHAMBERS

SUMMARY

This paper is concerned with the prediction and measurement of flow and heat transfer in motored diesel engine swirl chambers.

Measurements are mainly carried out by a temperature-compensated hot-wire anemometer and a high speed camera. Predictions are based on the solution of the finite-difference form of the governing differential equations for the transport of mass, momentum and energy by way of digital computers. In general, the obtained agreement between predictions and measurements is fairly good which confirms the accuracy of the described prediction procedure.

NOMENCLATURE

A_c	influence coefficient
A_p	equal to $\sum A_c$
C_u, C_1, C_2	Constant of the turbulence model
C_{pm}	mean piston velocity
h	total enthalpy
K	turbulence kinetic energy
m_c	mass flow rates across cell boundaries
M^o	equals to $(\rho V)_{p^o} / \delta t$ old values at time
M^h	equals to $(\rho V)_p^h / \delta t$ new values at time $t + \delta t$
p^o	pressure
p'	pressure correction
u	tangential velocity
\mathbf{u}	velocity vector at any point
r	radial position
S_p	coefficient of linearized source term
S_u	coefficient of linearized source term
S	source/sink term for variable ϕ
t	time
v	radial velocity
V	cell volume
β	equal to $(\partial \rho / \partial p)_T$
ϵ_ϕ	effective diffusivity coefficient for variable ϕ
ϵ	dissipative rate of turbulent kinetic energy
θ	angular position
ϕ	arbitrary dependent variable

μ laminar viscosity
 μ_{eff} effective viscosity
 ρ density
 $\sigma_h, \sigma_k, \sigma_\epsilon$ constants of turbulence model for h, K & ϵ .
 Σ_c summation for neighbouring nodes of typical grid node.

Subscripts.

E,W,N,S East, West, North and South neighbouring nodes
 e,w,n,s midway nodes between each node.

INTRODUCTION

The availability of very large, high speed digital computer has encouraged efforts to simulate the compression ignition engines. Complete mathematical model for the calculation of the heat release in a swirl chamber of a diesel engine is still not available. The heat release in multifuel engines depends to a great extent on the hydrodynamic mixing and transport processes, the fuel atomization and evaporation, the chemical reaction mechanism and reaction rates, heat transfer and environmental conditions, all of which vary inside the swirl chamber. The air-fuel mixing process prior to autoignition is important in diesel engine, in general and in swirl chamber diesel engine in particular. Moreover the mixing process controls combustion which in turn controls the rate of pressure rise, noise emission and pollutant formation in engine cylinders [1,2,3].* The study of pure phenomena in subclasses will help the solution of the more complex combustion phenomena resulting from multifuel combustion.

Therefore, a mathematical prediction model capable of predicting the air velocity inside swirl combustion chamber is required for the development of multifuel engines as well as saving time and cost.

There have been several experimental investigations, as a consequence of the development of swirl chambers; for the determination of the swirl chamber parameters. However, it was found that the study of flow is the more accurate method for determination of swirl chamber parameters. Theoretical investigations have been therefore reported [4,5,6]. Most of these investigations are based on the evaluation of the intensity of charge motion which relies in empirical correlations. Moreover, they are based on the application of evaluating parameters recommended from the analysis of the present

* A list of references is given at the end of the chapter.

swirl chambers. Such evaluating parameters have a quite wide range that they cannot give sufficient accurate results. Recently, ELKOTB [7] proposed a new theoretical model based on the equality of the moment of momentum resulting from the ejection velocity to the swirl chamber and the moment of momentum of the rotating air inside the swirl chamber provided that the air motion in the central zone is solid vortex and that in periphery is free vortex. This model can define the average velocity to the swirl chamber and the moment of momentum of the rotating air inside the swirl chamber provided that the air motion in the central zone is solid vortex and that in periphery is free vortex. This model can define the average velocity and can not facilitate the study of the interaction between fuel and air. Over the past decade a fairly considerable effort has been expended on computational procedures with the aid of mathematical models, for reciprocating engines [8,9,10]. These prediction procedures are based mainly on the solution of the finite difference for the governing differential equations for the transport of mass momentum and energy.

Although these attempts have been made to predict the properties of turbulent motion by mathematical models, no explicit consideration of the physical properties in swirl chamber is taken. These includes the continuous variation of the medium pressure and temperature and heat transfer during flow. Moreover, the shape of the combustion chamber with its effect on the air flow was not included.

The objective of this work is to develop a complete mathematical model of the prediction of the turbulent flow field in swirl chambers. Experimental measurement of the air flow velocity was planned to satisfy careful comparison over a wide range with the predicted values to obtain reliable information about the constants of turbulence model. Actually these constants depend on local turbulence values. This proposed prediction procedure is required to investigate speedily and with reasonable detail and accuracy the combustion of fuel with various chemical properties as well as the effect of various factors on the combustion process needed for the development of multifuel engines.

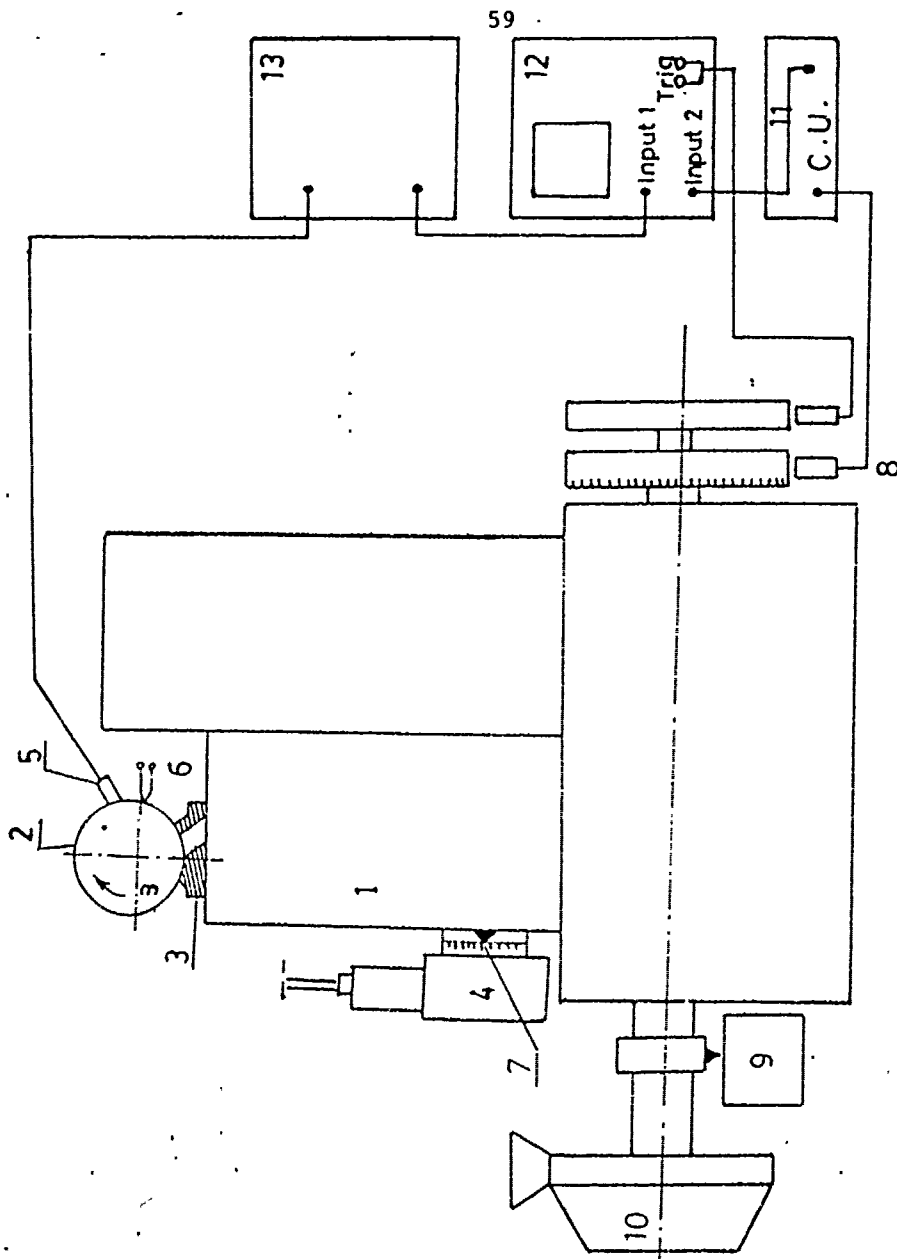
EXPERIMENTAL INVESTIGATION

A careful comparison over a wide range of data can give, in addition to the mean velocity field, reliable information about the constants of turbulence model. Therefore an experimental setup has been built up to facilitate measurements of

the air velocity components inside the swirl chamber with the highest possible accuracy. The experimental swirl chamber has been built up in one of the engine cylinders of a 2-cylinder, 4-stroke, water cooled medium speed diesel engine. The other cylinder has been used for motoring the engine to the required regime. The engine was directly coupled with hydraulic dynamometer for engine loading and equipped with various instruments required for measuring the main engine parameters.

The scope of this investigation includes the measuring of the instantaneous velocity components and finding out the effect of various constructional and working conditions on the air flow inside swirl chambers. For this reason the cylinder head was modified and a swirl chamber was constructed and attached instead of the original chamber. A Schematic drawing of the experimental setup is shown in Fig.(22). A cylindrical combustion chamber of 48.5 mm in diameter, Fig. (23) satisfying a relative swirl chamber volume ratio of 0.507 was constructed with an optically flat fused quartz window on one of its sides. The swirl chamber was built up with compression ratio 17. Two oblique washers were fitted on either sides of the quartz plate to avoid stress concentration. The quartz lens was fastened by a self locking screwed collar facilitating easy firm and quick assembly. The test swirl chamber was fitted with a cooling jacket supplied with glysrine from an independent circulating system to control its surface temperature. Connecting ports with various configurations were constructed to supply air to the swirl chamber from the main chamber. The chamber was designed such that variation of the relative swirl volume ratio [7], the connecting port area ratio [7] and the connecting port inclination angle are possible. The intake and exhaust manifolds of the test cylinder were separated from those of the second motoring cylinder.

The chamber was equipped with a temperature compensated hot wire anemometer to measure the air velocity components. The probe of the hot wire was connected to an ultraviolet oscillograph through the compensating bridge. It was equipped also with two ferrous-constantan thermocouples for measuring the surface temperature. The quartz window was used to photograph the air motion inside the swirl chamber with a high speed camera. The gas pressure, variations inside the main and swirl combustion chambers together with the crankangle were picked by a highly sensitive Piezo-electric transducers and an external X-generator. The display of the gas pressure was synchronised with the disc displaying the signal of the top dead centre. The data recorded during an engine



- 1 Engine Assembly.
- 2 Swirl Chamber.
- 3 Variable Area Port.
- 4 Inject. pump.
- 5 Hot wire anemometer
- 6 Thermocouples.
- 7 Advance Angle Adjustment
- 8 T.D.C. Pickup.
- 9 Tachometer.
- 10 Dynamometer.
- 11 Degree marker amplifier
- 12 Loop Oscillograph.
- 13 Balancing system.

Fig(22) Scheme Of Experimental Set up.For Air Flow Measurement

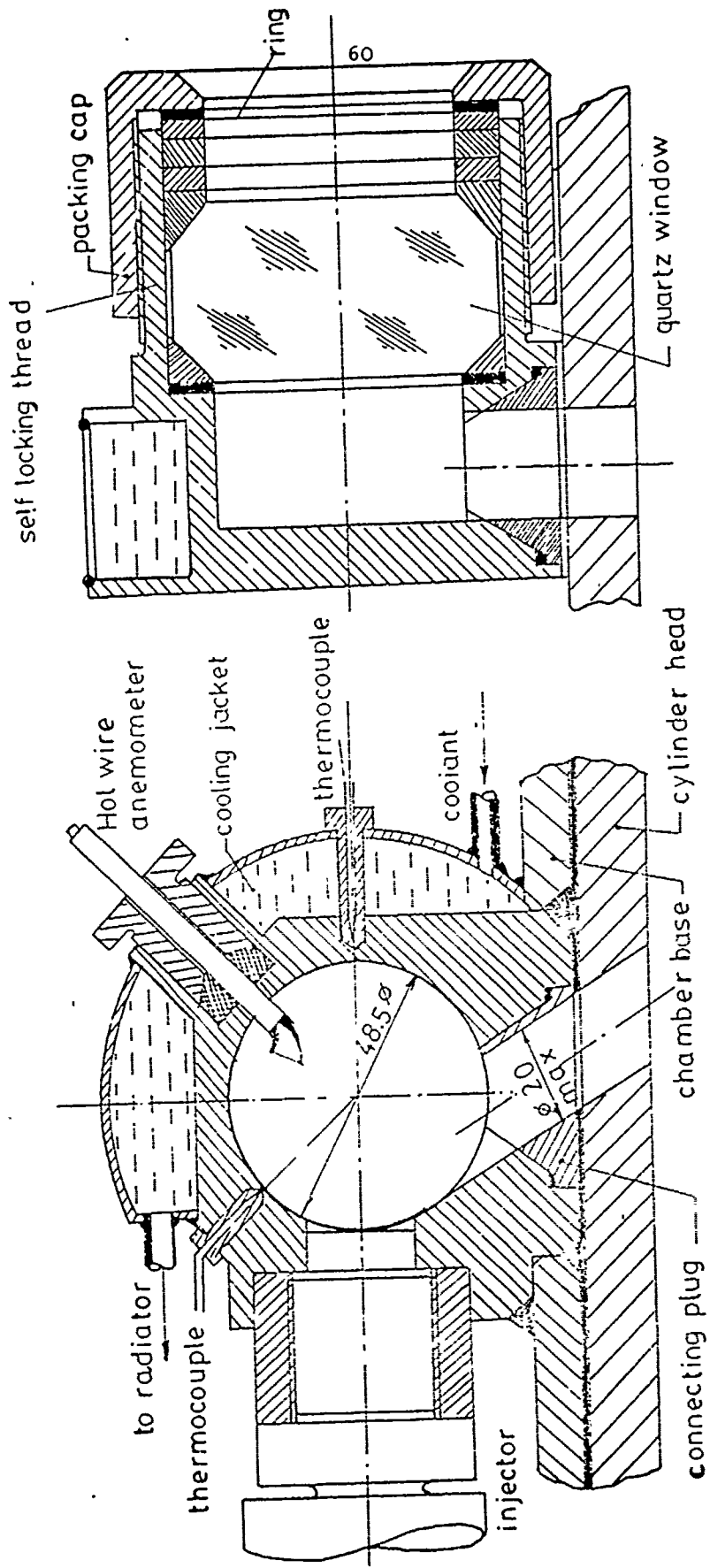


FIG.23 SCHEME OF THE TEST COMBUSTION CHAMBER FOR AIR FLOW MEASUREMENTS.

run included combustion chamber pressure, velocity variation for two inclination angles of the hot wire at each location, crank-angle, top dead centre and two surface thermocouples. Because of the cycle to cycle variations in data recorded and hence in air velocity components, it was required to examine a large quantity of data to obtain a quite sufficient reasonable results. Thus, a high speed multi channel data recording and processing system was applied. The output from the hot wire anemometer was magnified and recorded by a magnetic taperecorder. A calibration signal was recorded at the start of recording. Thereafter, the analog signal representing the air velocity variation at two inclination angles were played back at a lower speed to the analog/digital converter and digitized at every crank angle for 50 cycles. The output of the 50 cycles was then processed and an average cycle of the velocity variations was determined and recorded on magnetic tape in digital form for subsequent processing on digital computer to determine the mean velocity and the random velocity.

THE GOVERNING CONSERVATION EQUATIONS

The flow inside diesel engines swirl chambers is a transient turbulent flow. For the case of motored engines, thermal radiation may be neglected. The flow is, thus, governed by the differential conservation equations of energy, mass and momentum. In the present investigation, the swirl chamber is cylindrical and the flow may thus be assumed two-dimensional.

The equations governing the flow in a cylindrical swirl chamber of a diesel engine can be obtained by decomposing the velocity, pressure, density and enthalpy into a mean and a fluctuating value respectively [9,11].

The turbulent diffusion fluxes which appear in the governing equations are modeled using Boussinesq approach in terms of the mean-flow gradients and eddy diffusivities. These eddy diffusivities are determined by solving additional differential conservation equations for the time-averaged kinetic energy of turbulence k and its dissipation rate ϵ . This kind of model was originally developed for steady turbulent flows [12] and has been modified, to introduce compressibility effects by analogy with the laminar stress tensor, by RAMOS [9].

Within the above framework, the governing set of equations may be compactly represented in terms of a single general equation for an arbitrary dependent variable ϕ ;

$$\frac{\partial}{\partial t} (\rho\phi) + \frac{1}{r} \frac{\partial}{\partial r} (r\rho v\phi) + \frac{1}{r} \frac{\partial}{\partial \theta} (\rho u\phi) - \frac{1}{r} \frac{\partial}{\partial r} (r\Gamma_{\phi} \frac{\partial \phi}{\partial r}) - \frac{1}{r^2} \frac{\partial}{\partial \theta} (\Gamma_{\phi} \frac{\partial \phi}{\partial \theta}) = S_{\phi} \quad (1)$$

where ϕ stands for radial velocity v , tangential velocity u , total enthalpy h , k and ϵ , t is time, ρ is density, Γ_{ϕ} and S_{ϕ} are respectively the effective diffusivity coefficients and source/sink terms for variable ϕ . Equation (1) represents also the continuity equation by replacing ϕ by 1. The definition of Γ_{ϕ} and S_{ϕ} are given in table (1). In table (1) μ_{eff} is the effective viscosity which is given by;

$$\mu_{\text{eff}} = \mu + C_{\mu} \rho K^2 / \epsilon \quad (2)$$

where,

μ is the laminar viscosity, C_{μ} , C_1 , C_2 , σ_h , σ_k and σ_{ϵ} are constants of the turbulence model and are given in ref. [9,11] \vec{u} is the velocity vector at any point in the swirl chamber.

Table (1): Definitions of Γ_{ϕ} and S_{ϕ}

ϕ	Γ_{ϕ}	S_{ϕ}
v	μ_{eff}	$-\frac{\partial P}{\partial r} + \frac{1}{r} \frac{\partial}{\partial r} (r\mu_{\text{eff}} \frac{\partial v}{\partial r}) + \frac{1}{r} \frac{\partial}{\partial \theta} [\mu_{\text{eff}} (\frac{\partial u}{\partial r} - \frac{u}{r})]$ $+ \rho \frac{u^2}{r} - 2(\mu_{\text{eff}}/r^2) (v + \frac{\partial u}{\partial \theta}) - \frac{2}{3r} \frac{\partial}{\partial \theta} [r(\mu_{\text{eff}} \cdot \text{div}(\vec{u}) + \rho \cdot K)]$
u	μ_{eff}	$-\frac{1}{r} \frac{\partial P}{\partial \theta} + \frac{1}{r} \frac{\partial}{\partial r} [r\mu_{\text{eff}} (\frac{1}{r} \frac{\partial v}{\partial \theta} - \frac{u}{r})]$ $+ \frac{1}{r^2} \frac{\partial}{\partial \theta} [\mu_{\text{eff}} (\frac{\partial u}{\partial \theta} + 2v)] + (\mu_{\text{eff}}/r) \cdot (\frac{1}{r} \frac{\partial v}{\partial \theta} + \frac{\partial u}{\partial r})$ $- \mu_{\text{eff}} \frac{u}{r^2} - \rho \frac{uv}{r} - \frac{2}{3r} \frac{\partial}{\partial \theta} (\mu_{\text{eff}} \cdot \text{div}(\vec{u}) + \rho K)$
1	0	
h	$\mu_{\text{eff}}/\sigma_h$	$\frac{\partial P}{\partial t} + v \frac{\partial P}{\partial r} + \frac{u}{r} \frac{\partial P}{\partial \theta} + \text{small terms}$

$$\begin{aligned} \phi & \Gamma_{\phi} & S_{\phi} \\ K & \mu_{\text{eff}}/\sigma_k & G - \rho \epsilon \\ \epsilon & \mu_{\text{eff}}/\sigma_{\epsilon} & \frac{\epsilon}{K} (C_1 G - C_2 \rho \epsilon) \end{aligned}$$

$$G = \mu_{\text{eff}} \left[2 \left(\frac{1}{r} \frac{\partial u}{\partial \theta} + \frac{v}{r} \right)^2 + 2 \left(\frac{\partial v}{\partial r} \right)^2 + \left(\frac{1}{r} \frac{\partial v}{\partial \theta} + \frac{\partial u}{\partial r} - \frac{u}{r} \right)^2 \right] - \frac{2}{3} \text{div}(\mathbf{u}) + (\mu_{\text{eff}} \text{div}(\mathbf{u}) + \rho K)$$

BOUNDARY CONDITIONS

The imposition of the boundary conditions for diesel engine swirl chambers is not as straight-forward as it may seem. At chamber walls : the velocity components all obey the no slip conditions; the walls are insulated and hence the wall heat flux is taken equal to zero in this stage; the turbulence fluctuations and their dissipation rate are also zero. Wall functions are used for grid nodes adjacent to the chamber walls to avoid using many grid lines in the boundary sub-layer [13]. At the inlet plane, i.e. the tangential port which connects the swirl chamber with the main chamber, the inlet velocity, density and temperature vary with crank angle (or time). They are specified by solving an ordinary differential equation for the flow from the main chamber to the swirl chamber, or vice versa, through the tangential port, in the manner explained in ref. [14].

THE FINITE-DIFFERENCE EQUATIONS

For the purpose of deriving the finite-difference equations, the swirl chamber is overlaid with a grid of nodes, formed by the intersections of meridional lines and circles (Fig.(24) at which the scalar variables h, K, ϵ and P are stored; while the velocities are located mid-way between the pressures which drive them. Equation (1) is formally integrated over imaginary control volume or 'cell' surrounding each variable and for a time increment δt . The finite-difference approximation to equation (1) is written as ;

$$(A_p + M_p^o - S_p) \phi_p^n = \sum_c A_c \phi_c^n + M_p^o \phi_p^o + S_u \quad (3)$$

where,

$A_p = \sum_c A_c$, \sum_c denotes summation over the four neighbouring nodes of a typical grid node P , c denotes neighbouring node of a grid node P , 'o' and 'n' denote 'old' and 'new' and

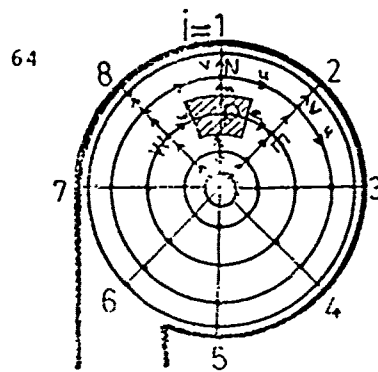


FIG.24 COMPUTATIONAL GRID.

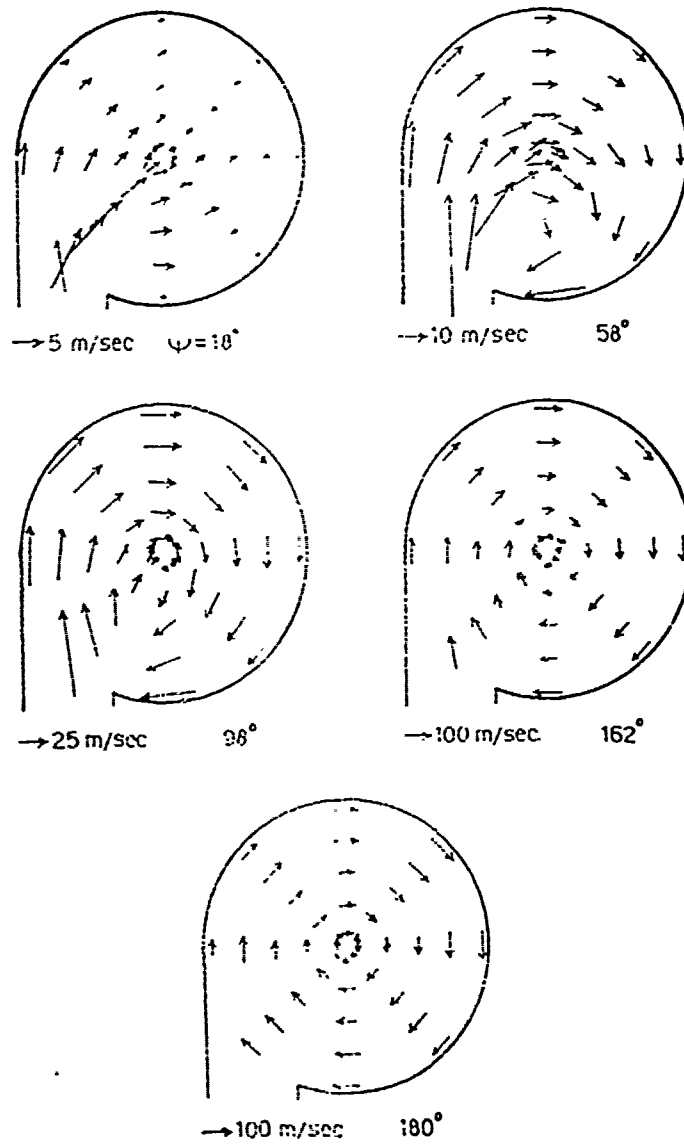


Fig.25 VELOCITY VECTOR FIELD DURING COMPRESSION STROKE

'new' values at times t and $t+\delta t$ respectively, M_p^0 equals $(\rho V)_p^0 / \delta t$, V is cell volume, S_p and S_u are coefficients of a linearized source term obtained by integrating S_ϕ . A_c are influence coefficients which give the combined effect of diffusion and convection.

The continuity equation is integrated to give ;

$$M_p^n - M_p^0 + \sum_c \dot{m}_c = 0 \quad (4)$$

where,

\dot{m}_c are mass flow rates across cell boundaries. Equation (3) can be solved for u, v, h, k and ϵ in space and time domains if the pressure field is known at each time step. The solution of Equation (3) may be obtained economically if coefficients A_c, S_p and S_u are computed at 'Old' time t and leaving ϕ_p^n and ϕ_c^n to be calculated in the 'new' time $t+\delta t$. This solution approach parallels that of a parabolic flow which is justifiable because equation (1) is indeed parabolic in time [15]. The set of difference equation (3) are linked through pressure differences terms.

OUTLINE OF THE SOLUTION PROCEDURE

At any instant of time t the ϕ^0 fields of the variables are known, predictions for a time increment δt are then obtained by solving the difference equations for the ϕ^n fields by a marching-integration algorithm. The latter then becomes the ϕ^0 for the prediction of the next time step; in this way the solution is marched forward in time until the desired period has been covered. The next section is devoted for the solution of the difference equations.

SOLUTION OF DIFFERENCE EQUATIONS

The energy equation is first solved, using the old fields of h, u, v, p and $(\partial p / \partial t)$, to yield the new enthalpy field (h^n) and hence the new temperature field (T^n).

The next step is to obtain a preliminary set of new velocity components v^{*n} and u^{*n} for an estimated new pressure field P^{*n} by solving their difference equations; P^{*n} is actually estimated as equal to the 'old' pressure P^0 .

The computed velocities v^{*n} and u^{*n} will not, in general, satisfy the local continuity equation (4) but will produce a net mass source at each grid node. The pressure, density and velocities are then corrected so as to reduce the mass source at each grid node to zero in the following manner ;

$$p^n = p^{*n} + p' \quad (5)$$

$$\rho^n = \rho^{*n} + \beta p' \quad (6)$$

$$v_p^n = v_p^{*n} + D_v (P'_p - P'_N) \quad (7)$$

$$u_p^n = u_p^{*n} + D_u (P'_p - P'_E) \quad (8)$$

where,

the * indicates guessed or preliminary value, P' is pressure correction, β is defined as $(\partial \rho / \partial P)_T$, D_v and D_u are evaluated from the relevant momentum equation, e.g. $D_u = u_p^n / (P_p - P_E)$, subscripts N and E denote neighbouring nodes, as shown in Fig. (24).

Equations (6-8) are substituted into the continuity equation (4) to give ;

$$(A_p - S_p) P'_p = \sum_C A_C P'_C + S_u \quad (9)$$

where,

$A_p = \sum_C A_C$, $S_u = -(M_p^{*n} - M_p^O + \sum_C m_C^*)$ is the local continuity imbalance based on u^{*n} , v^{*n} and ρ^{*n} ; S_p and A_C are coefficients which are defined as follows ;

$$S_p = -V_p \beta_p / \delta t - \sum_C (\beta_C \dot{m}_C^* / \rho_C^{*n}) \quad (10)$$

$$A_E = \rho_e^{*n} a_e D_{ue} - 0.5 \beta_e \dot{m}_e^* / \rho_e^{*n}; A_w = \rho_w^{*n} a_w D_{uw} + 0.5 \beta_w \dot{m}_w^* / \rho_w^{*n};$$

$$A_N = \rho_n^{*n} a_n D_{vn} - 0.5 \beta_n \dot{m}_n^* / \rho_n^{*n}; A_S = \rho_s^{*n} a_s D_{vs} + 0.5 \beta_s \dot{m}_s^* / \rho_s^{*n}$$

(11)

where,

subscripts E,W,N,S and e, w,n,s are neighbouring nodes and corresponding nodes mid-way between each node and a typical nodes P respectively (Fig.(24). In proving equation (9) terms involve P'^2 were ignored because P' itself should be small. It should be noted that the pressure correction equation does not include P' of 'old' time because there is no question of correcting 'old' velocities and pressure fields.

Equation (9) is solved to yield the P' field which is required to correct P, δ, v and u fields. The new K and ϵ are then computed from their difference equation (3).

OTHER FEATURES

The difference equations (3) & (9) are modified at cells adjoining the swirl chamber boundaries to incorporate the conditions imposed there. In addition to P' , a global pressure correction P' is computed based on overall continuity balance and is added to the existing pressure field before solving the pressure correction equation (11). The method of solution used to solve equations (3) & (9) is a Gauss-elimination line-by-line double-sweep technique. While equation (3) converges very fast, equation (9) needs more sweeps and some times more than one iteration to reduce the residual mass errors to an acceptable level. The modified form of the pressure correction equation, developed here, gives a fast convergence which reduces the total computational time. The time increment δt which is used in the present work is 2.22×10^{-4} s which is equivalent to 2° crank angle.

PREDICTION AND MEASUREMENT RESULTS

The computational grid inside the swirl chamber consists of 10 angular and 8 radial locations. Finer grid could be employed, at the expense of an increase in computational time; however the increase of number of grid nodes is not warranted at this stage. The computation is started at zero time, defined as the time at which the compression stroke has started. The inlet values to the swirl chamber are taken from the previous computational method, reported in [15]. Computations are carried out for a diesel engine with a swirl chamber of 48.5 mm diameter, tangential port of diameter 15 mm and inclined angle 45° to the cylinder axis, engine speed 1500 RPM, and compression ratio 17. The computations are carried at 2° crank angle intervals. The resulting velocity field computed at various times is shown in Figs (25) and (26) and the corresponding contours of the turbulence intensity distributions ($\sqrt{2k/3}/C_{pm}$, where C_{pm} is the mean piston velocity ($C = 7\text{m/s}$) is shown in Fig.(27).

In time sequence, one can observe the features of the flow evolution. At crank angle 18° , it can be seen that the air jet exists at the tangential port with a small velocity which is principally directed from both sides of the port to the opposite wall surface. The flow in the swirl chamber during the initial part of the compression stroke is almost pure radial flow. After some time for example at 58° crank angle, the pressure gradient that have built up at the opposite surface have already initiated rotational flow in the bulk of the swirl chamber. Before the initiation of the complete rotational flow a vortex is noticed at the right-hand side of the jet. Before the end of the compression stroke the radial pressure

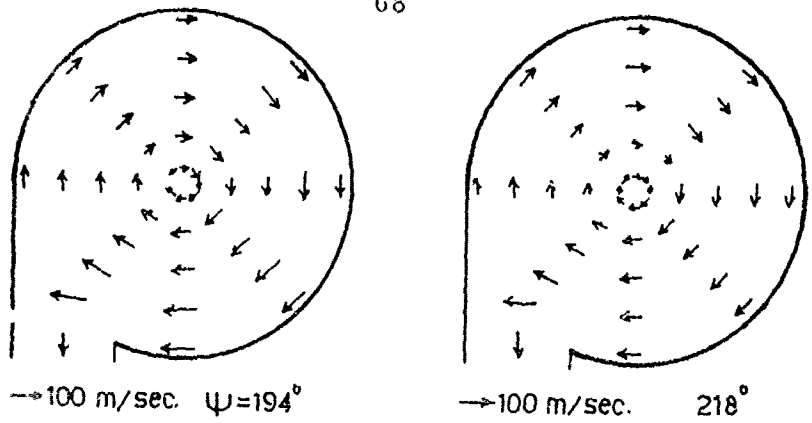


Fig.26 VELOCITY VECTOR PLOT DURING EXPANSION STROKE

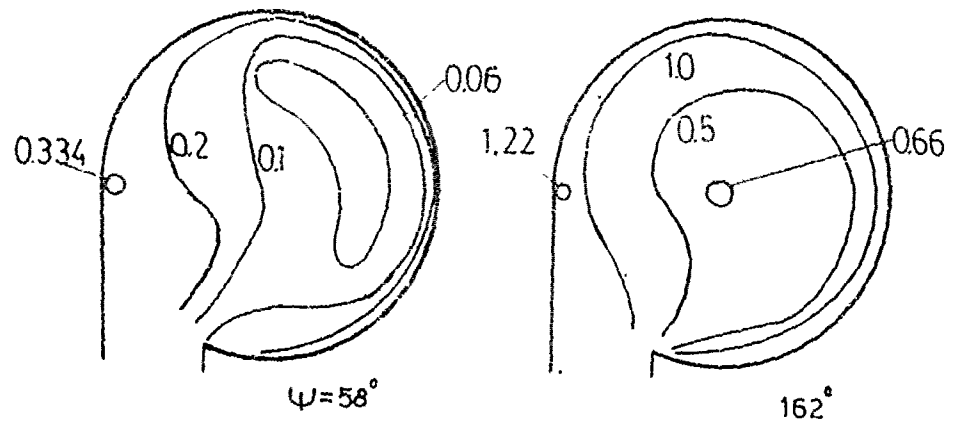


Fig.27 TURBULENT INTENSITY CONTOURS DURING COMPRESSION STROKE.



Fig.28 PHOTOGRAPHY OF THE FLOW FIELD AT T.D.C.

gradients have strengthened to the point of inducing strong flow recirculation which was observed from the high speed photographing of the flow field as shown in Fig. (28). The strong recirculating flow inside the swirl chamber produces a large tangential velocity component along the chamber surface and small tangential velocity component at the centre, as shown in Fig. (29). It is noticed also that the tangential velocity component increases during compression stroke reaching its maximum value at about 15° crank BTDC, as shown in Fig. (30). At the beginning of the expansion stroke the recirculating flow is unable to reverse its direction to flow through the tangential port in spite of the absence of a jet flow into the swirl chamber, as shown in Fig. (26). Before the complete reverse of the flow a vortex is noticed at the opposite side to the port. It should be mentioned that by this time, the flow velocities are low.

The turbulence contours during compression stroke are also shown in Fig. (27) in which it is noticed that the turbulence levels at the beginning of the compression stroke are low. By increase of time the inflow to the swirl chamber increases and separates at the beginning near to the tangential port to form eddies at either sides of the jet. Turbulence intensity generation is particularly strong reaching maximum value of 1.33 near to the entry port. Substantial decrease of the turbulence intensity has been obtained by BTDC where a complete recirculating flow is established. This decrease of turbulence intensity presumably being a consequence of the gradual reduction of the inflow rate by 12° crank angle as the piston approaches the end of the compression stroke.

Figure (31) shows the variation of the turbulence intensity along the radius (plane 2). Maximum turbulence intensity is noticed near chamber walls while the minimum intensity occurs at a radius of about 1.0 mm. Turbulence intensity variation, at 10 mm. from chamber walls with crank angle is depicted in Fig. (32). Turbulence intensity is very low at the beginning of compression. It then increases rapidly during the compression stroke reaching a maximum value at the end of compression where the turbulence intensity starts to decrease again during the expansion stroke.

Comparisons of measurements and predictions of tangential velocity in the swirl chamber with the probe located at 10 mm from the wall surface at plane 2 which is 45° to the port axis. The solid line represents the predicted values. A quite sufficient agreement is noticed BTDC as shown in Fig. (30) however discrepancy is noticed during the mid of the compression stroke, Fig. (31). This discrepancies may be attributed to

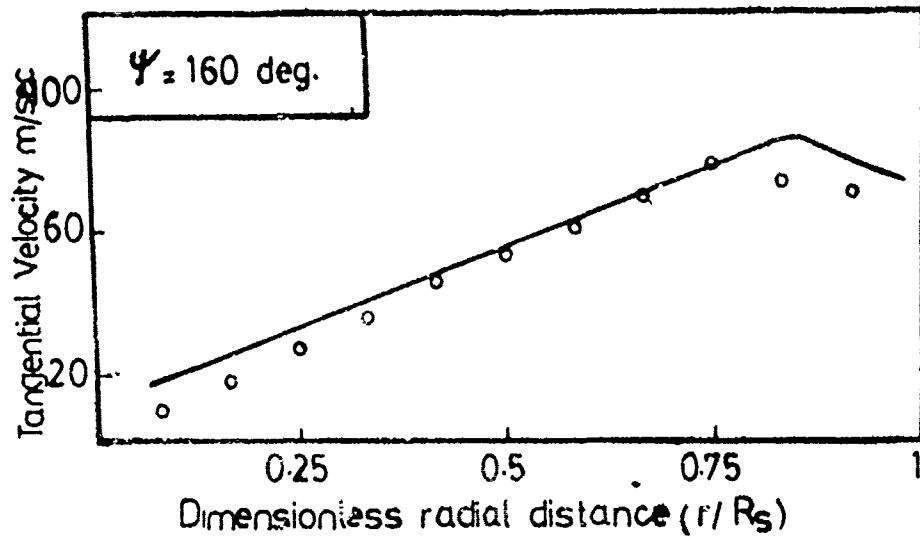


FIG. 29 PREDICTED AND MEASURED TANGENTIAL VELOCITY IN PLANE 2 AT VARIOUS RADII AT 200 BTDC

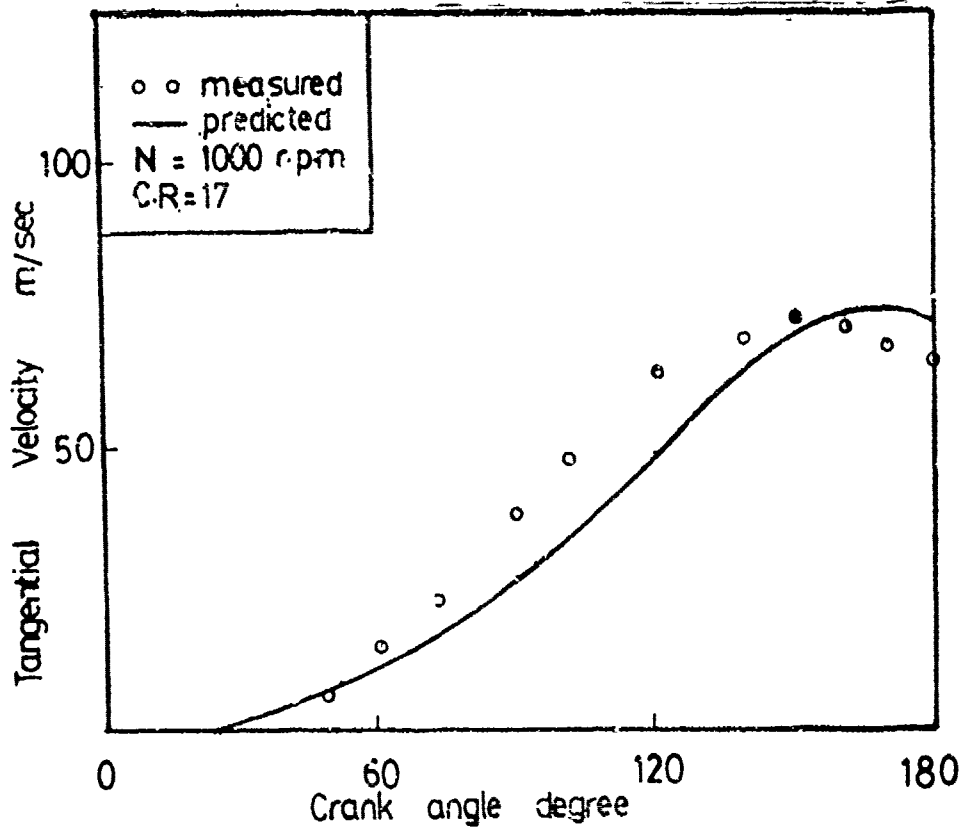


FIG. 30 PREDICTED AND MEASURED TANGENTIAL VELOCITY DURING COMPRESSION IN PLANE 2 AT 10 MM FROM INSIDE SURFACE.

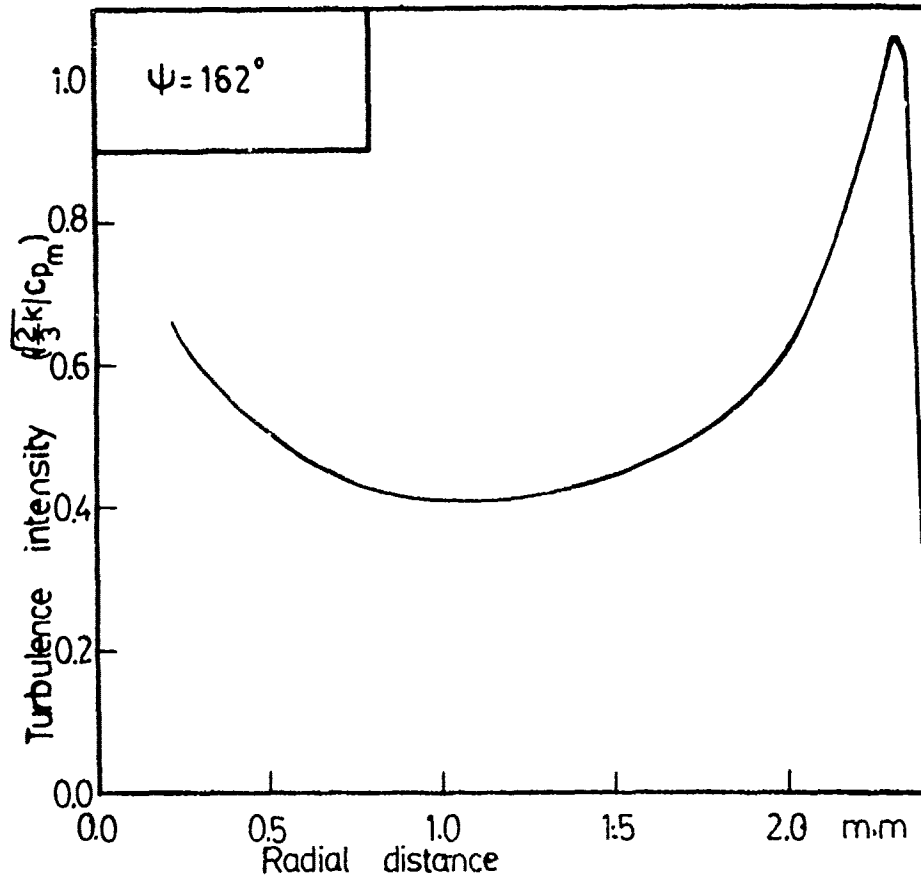


FIG. 31 RADIAL TURBULENCE INTENSITY DISTRIBUTION IN PLANE 2 AT 200° BTDC.

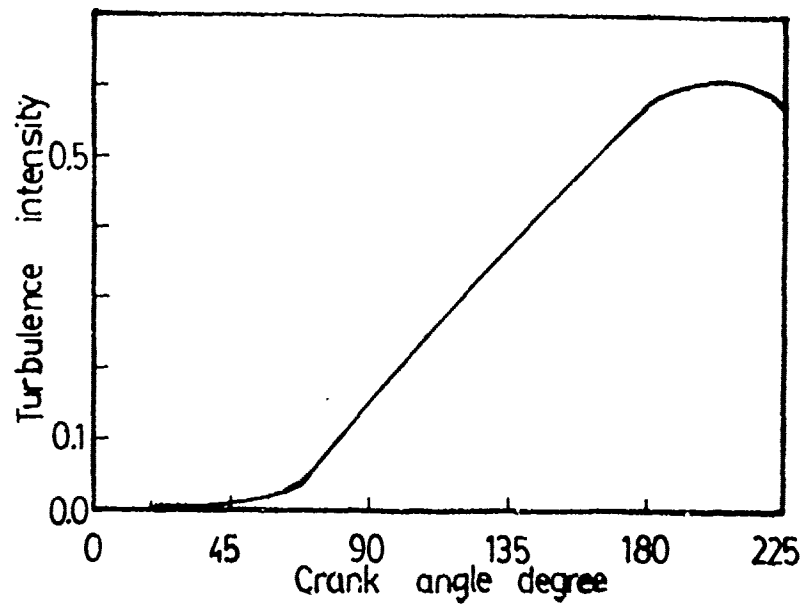


FIG. 32 TURBULENCE INTENSITY DURING COMPRESSION AT 10 MM FROM INSIDE SURFACE.

the error resulting from the determination of the inclination of the velocity vector by the hot wire anemometer. The measured values are clearly sensitive to this inclination angle which can be defined accurately after the circulating flow has been established.

It is planned to investigate the effect of various geometry parameters of the swirl chamber and working conditions on the flow field to isolate some of the important features of flow and to validate the computational procedure. The present work lays the framework for a more detailed study including spray mixing and combustion which might well prove helpful to the designer.

REFERENCES

- | 1 | VOICULESCU, I.A. and BORMAN, G.L. "An Experimental Study of Diesel Engine Cylinder-Averaged NO_x Histories" SAE Paper No. 780228, 1978.
- | 2 | PISCHINGER, F.F. and KLOCKER, J.J. "Single Cylinder Study of Stratified Charge Process with Prechamber Injection" SAE Paper No. 741162, 1974.
- | 3 | BONI, A.A. et al "Computer Simulation of Combustion Processes in a Stratified Charge Engine" ACTA ASTRONAUTICA, Vol. 3, No. 3-4. 1976.
- | 4 | FEDOTENKO, F.S. "The Effect of Swirl Chamber Volume on the Work of 4-Stroke Self-Ignition Engines" NAMU, Vol. 69, 1953.
- | 5 | BOTTGGER "Ursacher der Klappfrein Dieselerbrennung", Craft, No. 8, 1958.
- | 6 | KHOFAK, M.C "Investigation of Mixture Creation in Engines with Devided Swirl Combustion Chamber" Proceeding of the Science Technology Conference, Academy of Science USSR, Moscow 1960.
- | 7 | ELKOTB, M.M. et al "Theoretical Investigation of Velocity Air Pattern Inside the Swirl Chamber" Bull. of the Faculty of Engng, Cairo University, Paper 17, 1976.
- | 8 | GOSMAN, A.D. et al "Axisymmetric Flow in a Motored Reciprocating Engine" Proc. of Inst. of Mech. Engineers, Vol. 192, No. 11, pp. 213-223, 1978.
- | 9 | RAMOS, J.I. et al "Numerical Prediction of Axisymmetric Laminar and Turbulent Flows in Motored, Reciprocating Internal Combustion Engines" SAE Paper No. 790356, 1979.
- | 10 | DRANG, M.S. et al "The Prediction of Heat and Mass Transfer During Compression and Expansion in I.C. Engines, SAE Paper No. 760761, 1976.

- | 11 | GOSMAN, A.D. and WATKINS, W. "A Computer Prediction Method for Turbulent Flow and Heat Transfer in Piston/Cylinder Assemblies" Paper Presented at Symposium on Turbulent Shear Flows, Pennsylvania, April 1977.
- | 12 | LAUNDER, B.E. and SPALDING, D.B. "Mathematical Models of Turbulence" Academic Press, 1972.
- | 13 | GOSMAN, A.D. et al "Assessment of a Prediction Method for in-cylinder Processes in Reciprocating Engines" Proc. General Motors Research Symposium on Combustion Modelling in Reciprocating Engines, 1978.
- | 14 | ELKOTB, M.M. et al "Spray Behaviour Inside A Swirl Chamber of A Diesel Engine" Proc. of the 1st Conference of Mech. Power Engng, Feb. 1977. Cairo.
- | 15 | PATANKER, S.V. and SPALDING, D.B. "A Calculation Procedure For Heat, Mass and Momentum, Transfer in Three-Dimensional Parabolic Flows" Int. J. Heat Mass Transfer, Vol.15 pp. 1787-1806, 1972.

C O N C L U S I O N S

The multifuel engine must operate in the same way when using either clear fuels or mixtures with an arbitrary ratio. An analysis of the influence of physical properties of fuel on mixture creation, combustion and engine performance has been carried out. It is concluded that the delivery pressure must be increased to 1.5 up to 3 bar and an electric delivery pump which is independent on the drive from the engine must be used to limit the vapour lock. The injection pump must be equipped with an arrangement for changing the injected quantity in dependence of the fuel specific weight. Three types of combustion chambers, which are mainly precombustion chambers, are recommended to use in multifuel engines. The analysis leads to the necessary study of the turbulence motion of air in combustion chamber; heat transfer to the chamber and droplets, droplet size distribution, rate of fuel evaporation and the rate of chemical reaction. The study of the mentioned parameters are required to satisfy a sufficient accuracy of the spray modelling.

A series of experiments has been carried out on a special designed swirl chamber diesel engine to investigate the effect of swirl chamber geometry and operating conditions on the instantaneous surface heat transfer. It is concluded that the mean surface temperature decreases with the increase of engine speed and decrease of load, swirl chamber diameter and throat diameter of the tangential port. It is also found that the instantaneous heat transfer coefficient to the wall of the swirl chamber is described quite accurately by the following dimensionless equation;

$$Nu = 1.175 \times 10^{-4} Re^{0.5} Pr^{-0.4} Eu^{-1.5} (d_s/d_t)^{1.2}$$

It is concluded also that high engine speeds and greater values of swirl chamber diameter results in high heat transfer to walls.

A measuring technique and a prediction procedure for flow in motored diesel engines swirl chambers are presented. The prediction procedure is based on solving numerically the differential conservation equations for a transient turbulent flow with heat transfer. The obtained agreement between predictions and measurements is fairly good which confirms the accuracy of the prediction procedure. However, the prediction procedure is currently being tested for variables more relevant to turbulence modelling such as the turbulence intensity and the turbulent shear stresses.

UNCLASSIFIED

SECURITY CLASSIFICATION OF THIS PAGE (When Data Entered)

REPORT DOCUMENTATION PAGE		READ INSTRUCTIONS BEFORE COMPLETING FORM
1. REPORT NUMBER	2. GOVT ACCESSION NO. AD-A095 240	3. RECIPIENT'S CATALOG NUMBER
4. TITLE (and Subtitle) Spray Modelling for Multifuel Engines.	5. TYPE OF REPORT & PERIOD COVERED First Annual Tech. Mar 79-Apr 80	
	6. PERFORMING ORG. REPORT NUMBER	
7. AUTHOR(s) M. M. Elkotb	8. CONTRACT OR GRANT NUMBER(s) DAERO-79-G-0017	
9. PERFORMING ORGANIZATION NAME AND ADDRESS Cairo Center for Combustion Cairo U. Egypt	10. PROGRAM ELEMENT, PROJECT, TASK AREA & WORK UNIT NUMBERS 1T161102BH57-06	
11. CONTROLLING OFFICE NAME AND ADDRESS USARDSG-UK Box 65 FPO 09510	12. REPORT DATE July 80	
	13. NUMBER OF PAGES 74	
14. MONITORING AGENCY NAME & ADDRESS (if different from Controlling Office)	15. SECURITY CLASS. (of this report) UNCLASSIFIED	
	15a. DECLASSIFICATION/DOWNGRADING SCHEDULE	
16. DISTRIBUTION STATEMENT (of this Report) Approved for Public Release, Distribution Unlimited.		
17. DISTRIBUTION STATEMENT (of the abstract entered in Block 20, if different from Report) - - - - - -		
18. SUPPLEMENTARY NOTES		
19. KEY WORDS (Continue on reverse side if necessary and identify by block number) Spray Distribution (U) Fuel Injection (U) Swirl chamber (U) Heattransfer (U) Multifuel Engine (U) Fuel Atomization		
20. ABSTRACT (Continue on reverse side if necessary and identify by block number) The multifuel engine must satisfy the common requirements of all engines but in addition must be capable: (a) of combustion of liquid fuel of natural and synthetic origin of wide distillation range (+30°C-450°C) from gasoline to lubrication oils. (b) to preserve approximately the same power output and operating characteristics for all fuels. (c) of easy starting with all fuels. To achieve these goals it is important to optimize the air-fuel mixing process by proper design of a swirl chamber. The instantaneous surface heat transfer CONT. OVERLEAF		

in swirl combustion of various geometries has been determined under firing conditions.

An analysis of the influence of fuel properties, mixing and heat transfer is presently performed.

UNCLASSIFIED

SECURITY CLASSIFICATION OF THIS PAGE (When Data Entered)